

Abstract

Carbon dioxide (CO₂) is the most important greenhouse gas whose atmospheric loading has been significantly increased by anthropogenic activity leading to global warming. Accurate measurements and models are needed in order to reliably predict our future climate. This, however, has challenging requirements. Errors in measurements and models need to be identified and minimised.

In this context, we present a comparison between satellite-derived column-averaged dry air mole fractions of CO₂, denoted XCO₂, retrieved from SCIAMACHY/ENVISAT using the WFM-DOAS algorithm, and output from NOAA's global CO₂ modelling and assimilation system CarbonTracker. We investigate to what extent differences between these two data sets are influenced by systematic retrieval errors due to aerosols and unaccounted clouds. We analyse seven years of SCIAMACHY WFM-DOAS version 2.1 retrievals (WFMDv2.1) using the latest version of CarbonTracker (version 2010).

We investigate to what extent the difference between SCIAMACHY and CarbonTracker XCO₂ are temporally and spatially correlated with global aerosol and cloud data sets. For this purpose, we use a global aerosol data set generated within the European GEMS project, which is based on assimilated MODIS satellite data. For clouds, we use a data set derived from CALIOP/CALIPSO.

We find significant correlations of the SCIAMACHY minus CarbonTracker XCO₂ difference with thin clouds over the Southern Hemisphere. The maximum temporal correlation we find for Darwin, Australia ($r^2 = 54\%$). Large temporal correlations with thin clouds are also observed over other regions of the Southern Hemisphere (e.g. 43% for South America and 31% for South Africa). Over the Northern Hemisphere the temporal correlations are typically much lower. An exception is India, where large temporal correlations with clouds and aerosols have also been found. For all other regions the temporal correlations with aerosol are typically low. For the spatial correlations the picture is less clear. They are typically low for both aerosols and clouds, but dependent

AMTD

5, 2887–2931, 2012

SCIAMACHY WFM-DOAS XCO₂: comparison with CarbonTracker

J. Heymann et al.

Title Page

Abstract

Introduction

Conclusions

References

Tables

Figures

⏪

⏩

◀

▶

Back

Close

Full Screen / Esc

Printer-friendly Version

Interactive Discussion

on region and season, they may exceed 30 % (the maximum value of 46 % has been found for Darwin during September to November).

Overall we find that the presence of thin clouds can potentially explain a significant fraction of the difference between SCIAMACHY WFMDv2.1 XCO₂ and CarbonTracker over the Southern Hemisphere. Aerosols appear to be less of a problem. Our study indicates that the quality of the satellite derived XCO₂ will significantly benefit from a reduction of scattering related retrieval errors at least for the Southern Hemisphere.

1 Introduction

Since pre-industrial times, the concentration of the atmospheric greenhouse gas carbon dioxide (CO₂) has increased by about 36 % mainly as a result of anthropogenic activities such as fossil fuel combustion, land use change and cement production (Solomon et al., 2007). The increase of atmospheric CO₂ results in global warming with adverse consequences such as rising sea levels and an increase of extreme weather conditions. Our knowledge about the sources and sinks of CO₂ has large gaps (Stephens et al., 2007). A better knowledge is required for reliable climate prediction. Previous inverse modelling studies have shown that satellite observations of the vertical column of CO₂ or of its column-averaged dry air mole-fraction, XCO₂, can deliver important information on regional CO₂ surface fluxes, which currently cannot be provided by the sparse surface networks of very accurate ground based measurements (Rayner and O'Brien, 2001; Houweling et al., 2004; Miller et al., 2007; Chevallier et al., 2007). However, this requires highly accurate satellite retrievals. As shown by Chevallier et al. (2007) and Miller et al. (2007) especially regional biases need to be avoided as even biases of a few tenths of a ppm can harm the inversion.

The grating spectrometer SCIAMACHY (SCanning Imaging Absorption spectroMeter of Atmospheric CHartography) (Burrows et al., 1995; Bovensmann et al., 1999) on-board ENVISAT (ESA's ENVironmental SATellite), launched in 2002, and the Fourier transform spectrometer TANSO (Thermal And Near infrared Sensor for carbon

SCIAMACHY WFM-DOAS XCO₂: comparison with CarbonTracker

J. Heymann et al.

Title Page

Abstract

Introduction

Conclusions

References

Tables

Figures

⏪

⏩

◀

▶

Back

Close

Full Screen / Esc

Printer-friendly Version

Interactive Discussion



SCIAMACHY WFM-DOAS XCO₂: comparison with CarbonTracker

J. Heymann et al.

Title Page

Abstract

Introduction

Conclusions

References

Tables

Figures

⏪

⏩

◀

▶

Back

Close

Full Screen / Esc

Printer-friendly Version

Interactive Discussion

Observation) on-board GOSAT (Greenhouse gases Observing SATellite) (Yokota et al., 2004; Kuze et al., 2009), launched in 2009, are the only satellite instruments which observe backscattered near-infrared sunlight and provide measurements of CO₂ columns or XCO₂ with high sensitivity down to the Earth's surface (Buchwitz et al., 2005a,b, 2006, 2007; Houweling et al., 2005; Bösch et al., 2006; Barkley et al., 2006a,b,c, 2007; Schneising et al., 2008, 2011; Reuter et al., 2010; Yokota et al., 2004; Oshchepkov et al., 2008; Butz et al., 2009; Saito et al., 2009; Kuze et al., 2009; Yoshida et al., 2011; Morino et al., 2011) as needed for the regional CO₂ surface flux inversion application. For the period of mid 2002–March 2009, SCIAMACHY is the only satellite instrument which permits XCO₂ retrievals with high near-surface sensitivity. In addition to SCIAMACHY and GOSAT, OCO-2 (Orbiting Carbon Observatory-2) (Crisp et al., 2004; Bösch et al., 2011) and CarbonSat (Carbon Monitoring Satellite) (Bovensmann et al., 2010) are planned future satellite missions with the objective to provide additional constraints on natural CO₂ sources and sinks. Amongst CarbonSat's objectives is also the monitoring of strong localised anthropogenic CO₂ and CH₄ emissions, e.g. from coal-fired power plants and landfill sites (Bovensmann et al., 2010; Velazco et al., 2011).

In order to invert SCIAMACHY measurements to obtain XCO₂, several retrieval algorithms have been developed (Buchwitz and Burrows, 2004; Buchwitz et al., 2006, 2007; Barkley et al., 2006a; Bösch et al., 2006; Schneising et al., 2008, 2011; Reuter et al., 2010). One of them is the Weighting Function Modified - Differential Optical Absorption Spectroscopy (WFM-DOAS) retrieval algorithm (Buchwitz et al., 2000). The latest version is WFMDv2.1 (Schneising et al., 2011, 2012), which is based on a fast look-up-table scheme. WFMDv2.1 has been used to generate a global XCO₂ data set covering the years 2003–2009 (Schneising et al., 2011). This data set is analysed in this study.

An important error source for satellite retrievals is unaccounted or not fully accounted scattering by aerosols and clouds. The impact of aerosols and clouds on XCO₂ or CO₂ column retrievals has been investigated in several studies mostly using simulations (Tolton and Plouffe, 2001; O'Brien and Rayner, 2002; Kuang et al., 2002;

SCIAMACHY WFM-DOAS XCO₂: comparison with CarbonTracker

J. Heymann et al.

Title Page

Abstract

Introduction

Conclusions

References

Tables

Figures

⏪

⏩

◀

▶

Back

Close

Full Screen / Esc

Printer-friendly Version

Interactive Discussion

Dufour and Bréon, 2003; Buchwitz and Burrows, 2004; Christi and Stephens, 2004; Mao and Kawa, 2004; Buchwitz et al., 2005a; van Diedenhoven et al., 2005; Barkley et al., 2006a; Aben et al., 2006; Bril et al., 2007; Reuter et al., 2010) but also by analysis of measured data (Houweling et al., 2005; Schneising et al., 2008).

To minimise scattering related errors, full physics retrieval algorithms were developed which explicitly account for aerosols and clouds (Reuter et al., 2010, 2011; Butz et al., 2009, 2011). These algorithms are computationally very expensive. For SCIAMACHY, only initial results derived using these advanced algorithms are described in the peer-reviewed literature (Reuter et al., 2011). The largest multi-year global SCIAMACHY XCO₂ data set described in the peer-reviewed literature is the WFMDv2.1 XCO₂ data set of Schneising et al. (2011, 2012).

In this study, we present an investigation of the WFMDv2.1 2003–2009 XCO₂ data set which we compare with CarbonTracker XCO₂. We focus on identifying and quantifying systematic retrieval errors caused by aerosols and unaccounted clouds. Schneising et al. (2008) presented an initial assessment of XCO₂ errors resulting from aerosols and clouds mostly based on simulated retrievals using WFMDv1.0 retrievals. Here we analyse WFMDv2.1 retrievals from real satellite data and discuss comparisons with global aerosol and cloud data sets based on measurements. During our investigation we have identified a scan-angle-dependent bias of the WFMDv2.1 data product. To correct for this we have developed an empirical correction method, which is described in this manuscript.

This article is organised as follows: A short overview of the WFM-DOAS algorithm is given in Sect. 2 followed by an analysis of the sensitivity of the WFM-DOAS cloud detection algorithm in Sect. 3. The global data sets used in this study are described in Sect. 4. The scan-angle-correction method and the results of a comparison of scan-angle-corrected and uncorrected SCIAMACHY XCO₂ with CarbonTracker XCO₂ are presented in Sect. 5. The main part of this manuscript, a spatial and temporal correlation analysis of SCIAMACHY minus CarbonTracker differences with global aerosol and

cloud data sets, is presented in Sect. 6. Finally, a summary and conclusions are given in Sect. 7.

2 WFM-DOAS retrieval algorithm (v2.1)

The WFM-DOAS (WFMD) retrieval algorithm was developed at the University of Bremen (Buchwitz et al., 2000) and has been further improved continuously to meet the needs of the data user community (Buchwitz and Burrows, 2004; Buchwitz et al., 2005a,b; Schneising et al., 2008, 2009, 2011). A detailed description of its theoretical background can also be found in the publication of Rozanov and Rozanov (2010). For this study, we use the WFMDv2.1 data product described in Schneising et al. (2011).

Briefly, the retrieval algorithm works as follows: It uses two spectral fit windows, which cover the O₂-A absorption band from 755 nm to 775 nm and CO₂ absorption lines between 1558 nm and 1594 nm. SCIAMACHY measures these spectral regions in nadir viewing mode with a spatial resolution of typically 60 km by 30 km. The simultaneously retrieved O₂ column is used as a light path proxy for CO₂ to reduce the influence of scattering effects. WFMD is a least-squares method which scales pre-selected atmospheric vertical profiles. The logarithm of a linearised radiative transfer model is fitted to the logarithm of the measured sun-normalised radiance (see Eq. 1 of Schneising et al., 2008). The fit-parameters directly yield the desired vertical columns of CO₂ and O₂. The O₂ column is needed in order to obtain the dry air column required for the conversion of the CO₂ column into XCO₂ (Schneising et al., 2008), the final product of the WFMD algorithm. The SCIAMACHY XCO₂ algorithm not only has to be very accurate but also sufficiently fast in order to process the large amounts of data produced by SCIAMACHY. For this reason, a fast look-up-table (LUT) scheme has been developed to avoid computationally expensive radiative transfer (RT) simulations. The WFMD algorithm also includes a cloud detection algorithm, which flags cloudy ground pixels, and a surface albedo retrieval, which delivers the surface albedo of a ground

SCIAMACHY WFM-DOAS XCO₂: comparison with CarbonTracker

J. Heymann et al.

Title Page

Abstract

Introduction

Conclusions

References

Tables

Figures

⏪

⏩

◀

▶

Back

Close

Full Screen / Esc

Printer-friendly Version

Interactive Discussion



pixel. Binary quality flags (“good/bad”) are set a posteriori to identify successful retrievals. They are based on various criteria such as the quality of the spectral fits.

In this study, monthly means of the SCIAMACHY WFMDv2.1 XCO₂ Level 2 data product of Schneising et al. (2011) are used, which cover the time period 2003–2009.

5 For the investigation of SCIAMACHY minus CarbonTracker differences, we only used data from the time period 2004–2008. We do not use 2003 data because of instrumental issues at the beginning of 2003 (Schneising et al., 2011). We excluded 2009 because the aerosol reference data we are using is only available until mid 2009.

2.1 WFM-DOAS and aerosols

10 WFMD uses a constant aerosol vertical profile for the RT simulations which does not depend on time or location. Aerosol variability is taken into account as follows: (i) by using O₂ as proxy for the light path, (ii) by the low-order polynomial included in the WFMD spectral fits, which makes the retrieval insensitive to spectrally broadband radiance modifications resulting from, for example, aerosols, and (iii) by filtering out scenes contaminated by high loads of aerosols as identified using the SCIAMACHY Absorb-
15 ing Aerosol Index (AAI) (Tilstra et al., 2007) data product, which is sensitive to aerosol events such as desert dust storms, volcanic eruptions or smoke from forest fires.

Nevertheless, aerosols are still a possible source of errors. Schneising et al. (2008) performed simulations to estimate the impact of aerosols on the WFMDv1.0 XCO₂
20 retrievals using several aerosol scenarios. They concluded that aerosol related XCO₂ errors are typically below 1 %.

2.2 WFM-DOAS and clouds

As mentioned, clouds are an important error source for the XCO₂ data product retrieved from measurements of the upwelling solar electromagnetic radiation of the top of the
25 atmosphere. Consequently, cloud contaminated ground scenes have to be identified

SCIAMACHY WFM-DOAS XCO₂: comparison with CarbonTracker

J. Heymann et al.

Title Page

Abstract

Introduction

Conclusions

References

Tables

Figures

⏪

⏩

◀

▶

Back

Close

Full Screen / Esc

Printer-friendly Version

Interactive Discussion



and filtered out. For this purpose, WFM-DOAS includes a cloud detection algorithm, which is based on two cloud filtering criteria.

The first criterion, used to establish cloud free scenes, is based on subpixel information provided by SCIAMACHY's polarisation measurement device (PMD) 1. PMD 1 is mainly sensitive to radiation which is polarised perpendicular to the SCIAMACHY optical plane and covers the spectral ultraviolet A (UVA) region between 310 nm and 365 nm. The spatial resolution is approximately 15 km by 30 km (Bovensmann et al., 1999). In order to identify a cloud contaminated ground scene, the high cloud brightness in the UVA region is used. PMD 1 is one of seven SCIAMACHY PMD channels and has been selected because of its low sensitivity to surface albedo variations (Buchwitz et al., 2005a). If the normalised and solar zenith angle corrected PMD 1 signal exceeds a certain threshold, the ground pixel is classified as cloud contaminated (Buchwitz et al., 2005a).

The second criterion is based on a threshold for the retrieved O_2 column. The retrieved O_2 column has to be larger than 90% of the assumed a-priori O_2 column which is determined from surface height (pressure) and the known mixing ratio of O_2 (Schneising et al., 2008).

In the following section more details describing the cloud detection algorithm are presented along with a quantitative analysis of the sensitivity of this algorithm as needed for the purpose of this study.

3 Sensitivity of the WFM-DOAS cloud detection algorithm

In order to study the influence of clouds on WFMDv2.1 XCO_2 , we have to know "which clouds" remain after the application of the WFM-DOAS PMD 1 and O_2 based cloud detection algorithm. For this reason, the minimum detectable effective cloud optical depth (eCOD defined as cloud optical depth times cloud fractional coverage) ("detection threshold"), which can be detected using the WFMDv2.1 cloud detection algorithm, has been determined using simulations. In the following it is described how these

SCIAMACHY WFM-DOAS XCO_2 : comparison with CarbonTracker

J. Heymann et al.

Title Page

Abstract

Introduction

Conclusions

References

Tables

Figures

⏪

⏩

◀

▶

Back

Close

Full Screen / Esc

Printer-friendly Version

Interactive Discussion



PMD 1 and O₂ detection thresholds have been obtained and what their threshold values are.

The SCIAMACHY PMD signals are not yet absolutely radiometrically calibrated. To be able to determine the sensitivity of the PMD-based cloud detection algorithm using RT simulations, the PMD cloud detection threshold needs to be related to the corresponding radiance or sun-normalised radiance also called intensity. In the following it is explained how this has been achieved.

The PMD algorithm works as follows: The uncalibrated PMD 1 signal is normalised to a fixed maximum value and divided by the cosine of the solar zenith angle (SZA). If this reflectivity-like PMD signal, SR_{PMD}, exceeds a given threshold of SR_{PMD} = 0.7 for at least one PMD subpixel, the SCIAMACHY pixel is flagged as cloudy. The used maximum value and the threshold have been obtained by visual inspection of SCIAMACHY PMD images (Buchwitz et al., 2005a).

In order to simulate SR_{PMD} using RT simulations, we calibrated PMD 1, i.e. we have determined the corresponding intensity in absolute physical units. For this purpose we have used the calibrated SCIAMACHY nadir intensity spectra in the corresponding wavelength region (using channel 2, cluster 9, covering the region 320 nm–365 nm). As shown in Fig. 1, the relationship between the PMD 1 signal and the mean intensity as measured by SCIAMACHY's science channel in the UVA region is linear. As can also be seen, the intensity, R_{SCI}, which corresponds to the PMD threshold SR_{PMD} = 0.7 is R_{SCI} = 0.1074. This relationship has been used in the following to assess the sensitivity of the PMD-based cloud detection algorithm to various cloud scenarios using RT simulations.

Simulated O₂ column retrievals have been used to determine the sensitivity of the O₂ column based cloud detection algorithm. This cloud detection algorithm works as follows: If the deviation between the retrieved and the a-priori O₂ column, defined as $P_{O_2} = 1 - O_{2,\text{retrieved}}^{\text{col}} / O_{2,\text{a-priori}}^{\text{col}}$, is larger than P_{O₂} = 10 %, the corresponding SCIAMACHY pixel is flagged as cloudy. For the RT simulations of the SCIAMACHY spectra the SCIATRAN RT code (Rozanov et al., 2005) has been used.

**SCIAMACHY
WFM-DOAS XCO₂:
comparison with
CarbonTracker**

J. Heymann et al.

Title Page

Abstract

Introduction

Conclusions

References

Tables

Figures

⏪

⏩

◀

▶

Back

Close

Full Screen / Esc

Printer-friendly Version

Interactive Discussion



SCIAMACHY WFM-DOAS XCO₂: comparison with CarbonTracker

J. Heymann et al.

Title Page

Abstract

Introduction

Conclusions

References

Tables

Figures

⏪

⏩

◀

▶

Back

Close

Full Screen / Esc

Printer-friendly Version

Interactive Discussion

The RT simulations are based on a standard scenario with an ice cloud. This scenario has been defined as follows: cloud top height (CTH) 10 km, cloud geometrical thickness (CGT) 500 m and fractal ice particles based on a tetrahedron with an edge length of 50 μm . Aerosols are considered by a realistic aerosol scenario (see the OPAC background scenario described in Schneising et al., 2008, 2009).

Figure 2 shows simulated R_{SCI} and O_2 column differences between retrieved and a-priori columns, P_{O_2} , for different cloud fractional coverages (CFC) as a function of cloud optical depth (COD). The simulations are valid for a surface albedo of 0.1 and a solar zenith angle (SZA) of 40° . The red lines show the PMD and O_2 cloud detection thresholds. The sensitivity of the cloud detection algorithm for several cloud scenarios are shown by the intersection between the simulations and the (red) PMD and O_2 threshold lines. As can be seen, minimum effective COD, i.e. the cloud detection thresholds, are 0.89 for the PMD algorithm and 0.07 for the O_2 algorithm.

This analysis has been repeated for different combinations of albedo, SZA and CTH. The results of these simulations are summarised in Table 1, which lists the sensitivities for different cloud and surface scenarios in terms of the minimum detectable eCOD. The surface scenarios correspond to the albedos of grass (UVA: 0.03; O_2 -A: 0.46), water (UVA: 0.04; O_2 -A: 0.02), sand (UVA: 0.01; O_2 -A: 0.25) and snow (UVA: 0.97; O_2 -A: 0.92) estimated from the ASTER (Advanced Spaceborne Thermal Emission and Reflection Radiometer) spectral library version 2.0 (Baldrige et al., 2009) and from the Digital Spectral Library 06 of the US Geological Survey. In addition, a constant albedo of 0.1 has been used.

The simulations yield the following results: The PMD-based algorithm filters out thick clouds and bright surfaces in the UVA region like snow. The O_2 -column based algorithm is typically more sensitive especially to high thin clouds. It needs to be pointed out that this analysis is restricted to homogeneously cloud covered ground pixels as the focus of this study is on (horizontally extended) thin cirrus clouds. Because a SCIAMACHY main channel ground pixel includes several PMD subpixel, the PMD algorithm is typically more sensitive for cloud detection than indicated in Table 1. The PMD algorithm

enables to detect optically thick but spatially small (i.e. subpixel) clouds (Buchwitz et al., 2005a). This aspect is not considered in this study. Table 1 shows that the sensitivity of the filter algorithms depends on the scene and on the SZA. As can be seen, thin clouds with eCOD of approximately less than 0.1 may remain undetected. This means that although a pixel is classified as cloud free by the WFMD cloud detection algorithm it may be contaminated by optically thin clouds such as subvisual cirrus clouds.

4 Description of global reference data sets

In this section we describe global data sets which have been used for comparison with the SCIAMACHY WFMDv2.1 XCO₂ data product.

4.1 CarbonTracker XCO₂

In order to obtain estimates for CO₂ surface fluxes and global atmospheric CO₂ distributions from NOAA's (National Oceanic and Atmospheric Administration) highly accurate and precise greenhouse gas air sampling network, NOAA has developed the global CO₂ assimilation and modelling system CarbonTracker (Peters et al., 2007). For this study we use CarbonTracker version 2010 data of the years 2004–2008 obtained from <http://carbontracker.noaa.gov> for comparison with SCIAMACHY XCO₂. In order to consider the altitude sensitivity of the SCIAMACHY WFMD XCO₂ retrievals we apply the WFMD XCO₂ averaging kernels to the CarbonTracker CO₂ vertical profiles. These profiles are integrated vertically to obtain appropriate CarbonTracker XCO₂. The corresponding CarbonTracker seasonal XCO₂ averages are shown in Fig. 3. The daily CarbonTracker XCO₂ data set has been regridded on a 0.5° × 0.5° longitude/latitude grid and sampled like SCIAMACHY.

SCIAMACHY WFM-DOAS XCO₂: comparison with CarbonTracker

J. Heymann et al.

Title Page

Abstract

Introduction

Conclusions

References

Tables

Figures



Back

Close

Full Screen / Esc

Printer-friendly Version

Interactive Discussion



4.2 Global information on aerosols

For global information on aerosols we use a data set generated within the European GEMS (Global and regional Earth-system Monitoring using Satellite and in-situ data) project (Benedetti et al., 2009; Morcrette et al., 2009). The data set has been obtained from http://data-portal.ecmwf.int/data/d/gems_reanalysis/. It covers the years 2004–2008 and provides homogeneous and consistent aerosol information in 12 hourly time steps with full global coverage. The GEMS aerosol product is based on the assimilation of MODIS (MODerate resolution Imaging Spectroradiometer) (Barnes et al., 1998) aerosol information into a global model (Benedetti et al., 2009; Morcrette et al., 2009). For the analysis, the data set has been prepared to coincide temporally with SCIAMACHY by linear temporal interpolation. Ångström coefficients have been calculated using the original GEMS wavelengths (550 nm, 670 nm and 865 nm) and utilised to estimate aerosol optical depth (AOD) at 760 nm as needed for this study. The spatial resolution of the original data set is $1.125^\circ \times 1.125^\circ$. This data set has been regridded on a $0.5^\circ \times 0.5^\circ$ longitude/latitude grid as also done for the CarbonTracker XCO₂ as described above. Seasonal averages of the resulting AOD at 760 nm are shown in Fig. 4. For this study, the aerosol data have also been sampled like SCIAMACHY.

4.3 Global information on clouds

Global information on thin clouds derived from CALIOP (Cloud-Aerosol Lidar in Orthogonal Polarisation) on-board CALIPSO (Cloud-Aerosol Lidar and Infrared Pathfinder Satellite Observations) has been used in this study because CALIOP is sensitive to subvisual cirrus clouds (Vaughan et al., 2004; Winker et al., 2007, 2009). CALIPSO is a satellite in the A-Train constellation and was launched in April 2006. The CALIPSO data product (CAL_LID_L2_05kmCLay-Prov-V3-01) provides information on COD, CTH and CGT with a horizontal resolution of 5 km by 60 m. A two-year daytime data set has been used for this study (2007 and 2008).

AMTD

5, 2887–2931, 2012

SCIAMACHY WFM-DOAS XCO₂: comparison with CarbonTracker

J. Heymann et al.

Title Page

Abstract

Introduction

Conclusions

References

Tables

Figures

⏪

⏩

◀

▶

Back

Close

Full Screen / Esc

Printer-friendly Version

Interactive Discussion

SCIAMACHY WFM-DOAS XCO₂: comparison with CarbonTracker

J. Heymann et al.

Title Page

Abstract

Introduction

Conclusions

References

Tables

Figures

⏪

⏩

◀

▶

Back

Close

Full Screen / Esc

Printer-friendly Version

Interactive Discussion



The investigation of the sensitivity of the WFM-DOAS cloud detection algorithm presented in Sect. 3 showed that ground pixels classified cloud free may still be contaminated by thin clouds with an effective optical thickness of up to approximately $eCOD = 0.1$. Therefore, the CALIPSO data have been filtered for clouds with $COD = 0.1$ or less. Using averaging and interpolation, monthly maps of cloud parameters (COD , CTH and CGT) have been generated with global coverage and a spatial resolution of $0.5^\circ \times 0.5^\circ$. The CALIPSO data set only provides binary information about cloud coverage. Consequently, the relative frequency of cloud occurrence has been computed for every gridbox and is used as CFC data set. Using CALIPSO derived COD and CFC, $eCOD (= COD \cdot CFC)$ has been computed. The corresponding seasonal averages of CALIPSO derived $eCOD$ are shown in Fig. 5. In order to obtain daily cloud information without gaps, the monthly data are used as daily data in the respective month. These daily CALIPSO data are sampled in the same manner as the daily data of the other data sets. The monthly means of the years 2007–2008 are used for the years 2004–2006, where no CALIPSO data are available. Note that due to the interpolation and averaging of the CALIPSO data only statistical evidence can be given and the data set should not be used on single measurement scale.

5 Viewing geometry correction

During our investigation of the SCIAMACHY WFMDv2.1 XCO₂ data set we have found a scan-angle-dependent bias of this data product. As explained, WFM-DOAS uses a fast LUT approach to avoid time consuming RT simulations. In order to generate a manageable LUT, it is needed to limit the number of LUT elements. For this reason, the LUT was computed for exact nadir viewing conditions, i.e. only a constant viewing zenith angle (VZA), also referred to as line of sight (LOS) angle, of 0° is used. To correct for a scan-angle dependent air mass factor, a geometrical VZA correction has been implemented for the CO₂ and O₂ columns (Buchwitz and Burrows, 2004), but this

does not correct the XCO_2 , as this correction cancels out when the CO_2 to O_2 column ratio is computed.

As shown in Fig. 6 we have used simulated WFM-DOAS retrievals to investigate if the retrieved XCO_2 suffers from a scan-angle dependent bias. Figure 6 shows the systematic XCO_2 retrieval error as a function of VZA for different SZAs, albedos and AODs. As can be seen, the error can be as large as several ppm, especially for ground pixels with large positive VZAs (i.e. ground pixels west of the nadir position). As can also be seen, the simulations show a quadratic dependence of the systematic error on the VZA. The reason for this dependence can be unconsidered atmospheric scattering related effects.

We have analysed the SCIAMACHY retrievals based on real satellite data to find out if this error can also be observed in the WFMDv2.1 XCO_2 data product. Figure 7 shows that this is the case. Figure 7a shows global, northern and southern hemispheric WFMDv2.1 XCO_2 for the years 2003–2009 as a function of the VZA. The 2D-histograms show the expected quadratic relation between the XCO_2 and the VZA. We found similar result also for smaller regions (not shown here). As can also be seen, the magnitude of the difference between the most westwards and most eastwards XCO_2 amounts to several ppm and is on the same order of magnitude as also found using simulations (see above).

In the next subsection, we present a method to correct for this bias. In the following, the original, i.e. uncorrected, SCIAMACHY XCO_2 data set is denoted as XCO_2^S , the scan-angle-corrected SCIAMACHY XCO_2 is denoted $XCO_2^{S^*}$ and the CarbonTracker XCO_2 is denoted XCO_2^C .

5.1 Correction method

Here we present an empirical scan-angle-bias correction scheme for the WFMDv2.1 data product.

SCIAMACHY WFM-DOAS XCO_2 : comparison with CarbonTracker

J. Heymann et al.

Title Page

Abstract

Introduction

Conclusions

References

Tables

Figures

⏪

⏩

◀

▶

Back

Close

Full Screen / Esc

Printer-friendly Version

Interactive Discussion



SCIAMACHY WFM-DOAS XCO₂: comparison with CarbonTracker

J. Heymann et al.

Title Page

Abstract

Introduction

Conclusions

References

Tables

Figures

⏪

⏩

◀

▶

Back

Close

Full Screen / Esc

Printer-friendly Version

Interactive Discussion

SCIAMACHY scans in nadir mode across-track with viewing zenith angles (VZA) between $\pm 32^\circ$ covering a total swath width of about 960 km. The VZA as given in the WFMDv2.1 Level 2 data product is between 0° and 32° , i.e. it is a non-negative number. The negative VZAs shown in Fig. 7 correspond to relative azimuth angles less than 100° (note that the azimuth angle is also given in the WFMDv2.1 XCO₂ L2 data product and that the SZA is less than 75° for WFMD after quality filtering). Negative VZAs correspond to ground pixels east of the nadir position (“east pixel”), positive VZAs correspond to ground pixels west of the nadir position (“west pixel”).

A quadratic function depending on the (signed) VZA is fitted to XCO₂^S. We have also tried other functions, e.g. a simple linear function, but a quadratic function fits best. The fit shown as blue curve in Fig. 7a is used to correct XCO₂^S in the following way:

$$\text{XCO}_2^{\text{S}^*} = \text{XCO}_2^{\text{S}} + \Delta\text{XCO}_2^{\text{S}^*-\text{S}} \quad (1)$$

$$\Delta\text{XCO}_2^{\text{S}^*-\text{S}} = C1 + C2 \cdot (\text{VZA} - C3)^2. \quad (2)$$

The VZA is given in degree and XCO₂ in ppm. The numerical values of the three parameters are: $C1 = 7$ ppm, $C2 = -0.003 \frac{\text{ppm}}{\text{deg}^2}$ and $C3 = -47.3$ deg. They have been obtained from the global fit result (shown in Fig. 7a). The quality of this method is analysed in the next section.

5.2 Results

The scan-angle-bias corrected XCO₂ is shown in Fig. 7b. As can be seen, the dependency of XCO₂ on the VZA is reduced considerably, both on global (a reduction of the range of the scan-angle-dependent bias from ± 9 ppm to ± 1 ppm) and on hemispheric scales.

In order to investigate if the scan-angle-bias correction improves the SCIAMACHY WFMdV2.1 XCO₂ data set also on smaller scales, a regional comparison of corrected and uncorrected XCO₂ with CarbonTracker has been performed.

SCIAMACHY WFM-DOAS XCO₂: comparison with CarbonTracker

J. Heymann et al.

Title Page

Abstract

Introduction

Conclusions

References

Tables

Figures

⏪

⏩

◀

▶

Back

Close

Full Screen / Esc

Printer-friendly Version

Interactive Discussion

For this purpose, we have defined sixteen regions, which are shown in Fig. 8 and listed in Table 2. Monthly means of the difference between SCIAMACHY WFMDOAS v2.1 XCO₂ and CarbonTracker XCO₂ ($\Delta\text{XCO}_2^{\text{S-C}}$) are used to determine the influence of the scan-angle-bias correction. Figure 9 shows the impact of the scan-angle-bias correction on $\Delta\text{XCO}_2^{\text{S-C}}$ for Southern Africa. As can be seen, the time series of $\Delta\text{XCO}_2^{\text{S-C}}$ (red curve with corrected XCO₂) and $\Delta\text{XCO}_2^{\text{S-C}}$ (black curve with uncorrected XCO₂) differ by up to about 1 ppm and show a significant correlation (linear correlation coefficient $r = 0.89$). The correlation coefficient between $\Delta\text{XCO}_2^{\text{S-S}}$ and $\Delta\text{XCO}_2^{\text{S-C}}$ is also large (-0.76). The standard deviation of the difference to CarbonTracker is smaller for the corrected (1.05 ppm) than for the uncorrected XCO₂, i.e. the agreement with CarbonTracker is better for the corrected XCO₂ for this region. The variances of the standard deviations show that about 50% of the variance of $\Delta\text{XCO}_2^{\text{S-C}}$ can be explained by the scan-angle-bias for this region.

The corresponding results for the other regions are shown in Table 3. The time dependence of $\Delta\text{XCO}_2^{\text{S-C}}$ is similar as $\Delta\text{XCO}_2^{\text{S-C}}$ for all regions. This is shown by the large correlation coefficients which are between 0.68 and 0.99. The correlation with $\Delta\text{XCO}_2^{\text{S-S}}$ is large for many regions, but for several northern hemispheric regions very small and/or non-significant. An example is China, shown in Fig. 10, where the large difference to CarbonTracker cannot be explained by the scan-angle related bias. The global correlation and standard deviation shows that the scan-angle-correction affects the XCO₂ data set mostly on smaller regional scales. The standard deviations of XCO₂ are improved using the correction over all southern hemispheric regions and for most northern hemispheric regions.

To further quantify the improvements due to the scan-angle-bias correction we computed the standard deviation of all XCO₂ single ground pixel measurement within a radius of 350 km around several locations for each month. The location of these sites are shown in Fig. 8 and listed in Table 4. The mean values of these standard deviations may be interpreted as an upper limit of the single measurement precision (random

**SCIAMACHY
WFM-DOAS XCO₂:
comparison with
CarbonTracker**

J. Heymann et al.

Title Page

Abstract

Introduction

Conclusions

References

Tables

Figures

◀

▶

◀

▶

Back

Close

Full Screen / Esc

Printer-friendly Version

Interactive Discussion



error). The real precision is likely smaller because the standard deviations are not only due to instrument and retrieval noise but also affected by real atmospheric XCO₂ variability (note that variations due to the seasonal cycle have largely been filtered out but using standard deviations of all data in a given month) and varying systematic errors, e.g. due to the scan-angle-dependent bias. Table 4 shows absolute (in ppm) and relative (percentage) standard deviations of WFMDv2.1 XCO₂ with and without scan-angle-bias correction. As can be seen, the standard deviation is somewhat smaller for the scan-angle-bias corrected data for all locations. The standard deviation of XCO₂ is on average 9.04 ± 1.51 ppm for the uncorrected data and is reduced to 7.42 ± 1.29 ppm for the corrected data.

Schneising et al. (2012) validated the scan-angle-corrected SCIAMACHY XCO₂ data product against FTS (Fourier transform spectrometer) measurements of TCCON (Total Carbon Column Observing Network). They found a regional precision of 2.1 ppm and a regional accuracy of 1.1 ppm. However, the difference to the validation results of the uncorrected XCO₂ data is not significant.

6 Analysis of SCIAMACHY-CarbonTracker XCO₂ differences due to aerosols and thin clouds

6.1 Analysis method

The three global data sets described in Sects. 4 and 5 have been used for a temporal and spatial correlation analysis: (i) the scan-angle-bias corrected SCIAMACHY-CarbonTracker difference, denoted XCO₂^{S⁺-C}, (ii) the AOD at 760 nm as derived from the GEMS aerosol product, and (iii) CALIPSO derived eCOD.

Monthly averages are the input for the temporal correlation analysis. For the spatial analysis, averages of the four meteorological seasons (DJF, MAM, JJA and SON) of the five years 2004–2008 are used instead of monthly averages for better spatial coverage

and to reduce the scatter of the satellite data. In addition, the resolution has been reduced to $1^\circ \times 1^\circ$ for the spatial analysis.

In order to test whether a correlation is significant or not, a t-test is being performed. For this reason, a test statistic t' based on the number of the data points n and the correlation coefficient r is computed:

$$t' = \frac{r \sqrt{n - 2}}{\sqrt{1 - r^2}}. \quad (3)$$

To decide whether the correlation coefficient is significant or not, the resulting t' is compared with the t from a t-table, $t(f, p)$, which depends on the degree of freedom $f = n - 2$ and the probability value p . p is the probability that the correlation is statistically firm and is set to 95%. If t' is larger than $t(f, p)$, the correlation coefficient is regarded to be significant.

6.2 Analysis results

The results of the temporal and spatial correlation analysis for China are shown in Fig. 11. The amplitude of the seasonal cycle is larger for SCIAMACHY compared to CarbonTracker. To a minor extent ($r^2 = 9.2\%$), the difference may be due to retrieval errors caused by thin clouds. The spatial analysis shows that in autumn 33% of the variability of $\Delta XCO_2^{S^+ - C}$ may be explained by eCOD, i.e. clouds related retrieval errors. The AOD over China is the highest of all investigated regions, therefore one would expect to find also the largest correlation. However, this analysis only shows low temporal and spatial correlations with aerosols. This may indicate that aerosols are not a significant problem for the WFMDv2.1 algorithm in this region. On the other hand it needs to be considered that CarbonTracker is not perfect. For example, there are indications that the underlying CASA (Carnegie-Ames Stanford Approach) biosphere model underestimates the net ecosystem exchange (NEE) between the atmosphere and the biosphere (Yang et al., 2007; Schneising et al., 2011; Keppel-Aleks et al., 2012).

SCIAMACHY WFM-DOAS XCO₂: comparison with CarbonTracker

J. Heymann et al.

Title Page

Abstract

Introduction

Conclusions

References

Tables

Figures

◀

▶

◀

▶

Back

Close

Full Screen / Esc

Printer-friendly Version

Interactive Discussion



**SCIAMACHY
WFM-DOAS XCO₂:
comparison with
CarbonTracker**

J. Heymann et al.

Title Page

Abstract

Introduction

Conclusions

References

Tables

Figures

◀

▶

◀

▶

Back

Close

Full Screen / Esc

Printer-friendly Version

Interactive Discussion



Figure 12 shows the corresponding results for Southern Africa. As can be seen, the amplitude of the difference is about 4 ppm. Neither a “U-shape”, as mentioned by Schneising et al. (2008) for the seasonal cycle of the southern hemispheric WFMdV1.0 XCO₂, nor an evident phase shift between the seasonal cycle of XCO₂^{S*} and XCO₂^C can be seen in this region. However, Fig. 12 shows that 31% of the temporal variability of $\Delta\text{XCO}_2^{\text{S}^*-\text{C}}$ may be explained by thin clouds. The temporal correlation of $\Delta\text{XCO}_2^{\text{S}^*-\text{C}}$ with aerosols is statistically not significant in this region. The spatial correlation analysis shows that there are some correlations between $\Delta\text{XCO}_2^{\text{S}^*-\text{C}}$ and eCOD and also with AOD. The largest influence of clouds and aerosols on the difference is during spring (MAM).

The corresponding results of the spatial and temporal correlation analysis for all regions investigated are summarised in Table 5. Many regions over the Northern Hemisphere show low spatial correlations ($r^2 < 25\%$). However, e.g. Africa, shows large correlations with thin clouds during spring (MAM). For the Southern Hemisphere, the spatial correlations often exceed 25%. The largest spatial correlation is found for Australia (48% during DJF).

Temporal correlations with eCOD are typically high for several regions over the Southern Hemisphere and typically low over the Northern Hemisphere with the exception of India. This corroborates the assumption of Schneising et al. (2011) that the differences between SCIAMACHY WMFDv2.1 and CarbonTracker XCO₂ over the Southern Hemisphere is likely due to unaccounted thin clouds. The low correlation with aerosols for many regions shows that aerosols likely only marginally contribute to the observed difference to CarbonTracker.

7 Summary and conclusions

In this manuscript, we presented a comparison between SCIAMACHY WFM-DOAS XCO₂ and output from NOAA’s assimilation and modelling system CarbonTracker to

SCIAMACHY WFM-DOAS XCO₂: comparison with CarbonTracker

J. Heymann et al.

Title Page

Abstract

Introduction

Conclusions

References

Tables

Figures

⏪

⏩

◀

▶

Back

Close

Full Screen / Esc

Printer-friendly Version

Interactive Discussion

find out to what extent the observed differences between these two CO₂ data sets are influenced by systematic retrieval errors due to aerosols and unaccounted (thin) clouds. For this reason, we used the WFMDv2.1 SCIAMACHY XCO₂ data product of Schneising et al. (2011) which covers the years 2003–2009 and CarbonTracker version
5 2010 obtained from NOAA.

During our investigation, we found a scan-angle-dependent bias of the WFMDv2.1 XCO₂ data product. We developed an empirical correction scheme based on a parabolic function. We showed that this correction removes the scan-angle-dependent bias to a large extent and also typically results in a better agreement with Carbon-
10 Tracker. We recommend to users of this data product to also apply the proposed correction scheme in order to improve the quality of the SCIAMACHY WFMDv2.1 XCO₂ data product.

We investigated to what extent the SCIAMACHY minus CarbonTracker XCO₂ differences are spatially and temporally correlated with global aerosol and cloud data sets. For this purpose, we used a global aerosol data set generated within the European
15 GEMS project, which is based on assimilated MODIS satellite data. For clouds, we used a data set derived from CALIPSO/CALIOP.

We found significant temporal correlations between the SCIAMACHY and CarbonTracker XCO₂ difference and CALIPSO/CALIOP effective cloud optical depth (eCOD)
20 over the Southern Hemisphere (e.g. up to $r^2 = 54\%$ over Darwin, Australia). Over the Northern Hemisphere the temporal correlations with eCOD were lower or non-significant (with one exception, India, where $r^2 = 68\%$). Temporal correlations with aerosol optical depth (AOD) were typically lower compared to eCOD or non-significant. The spatial correlation analysis showed no clear picture over the Northern Hemisphere.
25 Over the Southern Hemisphere, spatial correlations with clouds were often larger than 25% (maximum: 48% during DJF over Australia).

The correlation with thin clouds over the Southern Hemisphere corroborates the conclusion of Schneising et al. (2011) that the seasonal cycle of WFMDv2.1 XCO₂ over the Southern Hemisphere presumably suffers from unconsidered scattering due to thin

clouds. This study provided more quantitative evidence that the quality of the SCIAMACHY WFM-DOAS-derived XCO₂ data product will benefit from algorithm improvements aiming at reducing cloud related retrieval errors as described in Heymann et al. (2012) by applying an improved cloud filtering and correction method.

5 *Acknowledgements.* CarbonTracker version 2010 data were provided by NOAA ESRL, Boulder, Colorado, USA, via the website at <http://carbontracker.noaa.gov>. We thank the European GEMS project for the global aerosol data set. We also thank the NASA Langley Research Center Atmospheric Science Data Center for providing us with the CALIOP/CALIPSO data. The research leading to the results presented in this manuscript has received funding from the European Union's Seventh Framework Programme (FP7) under Grant Agreements no. 212095 (CityZen) and 218793 (MACC), ESA (ADVANSE, CARBONGASES, GHG-CCI, SQWG), DLR (SADOS) and the University and the State of Bremen.

References

- 15 Aben, I., Hasekamp, O., and Hartmann, W.: Uncertainties in the space-based measurements of CO₂ columns due to scattering in the Earth's atmosphere, *J. Quant. Spectrosc. Ra.*, 104, 450–459, doi:10.1016/j.jqsrt.2006.09.013, 2006. 2891
- Baldrige, A. M., Hook, S., Grove, C., and Rivera, G.: The ASTER Spectral Library Version 2.0, *Remote Sens. Environ.*, 113, 711–715, doi:10.1016/j.rse.2008.11.007, 2009. 2896
- 20 Barkley, M. P., Frieß, U., and Monks, P. S.: Measuring atmospheric CO₂ from space using Full Spectral Initiation (FSI) WFM-DOAS, *Atmos. Chem. Phys.*, 6, 3517–3534, doi:10.5194/acp-6-3517-2006, 2006a. 2890, 2891
- Barkley, M. P., Monks, P. S., and Engelen, R. J.: Comparison of SCIAMACHY and AIRS CO₂ measurements over North America during the summer and autumn of 2003, *Geophys. Res. Lett.*, 33, L20805, doi:10.1029/2006GL026807, 2006b. 2890
- 25 Barkley, M. P., Monks, P. S., Frieß, U., Mittermeier, R. L., Fast, H., Körner, S., and Heimann, M.: Comparisons between SCIAMACHY atmospheric CO₂ retrieved using (FSI) WFM-DOAS to ground based FTIR data and the TM3 chemistry transport model, *Atmos. Chem. Phys.*, 6, 4483–4498, doi:10.5194/acp-6-4483-2006, 2006c. 2890

SCIAMACHY WFM-DOAS XCO₂: comparison with CarbonTracker

J. Heymann et al.

Title Page

Abstract

Introduction

Conclusions

References

Tables

Figures

⏪

⏩

◀

▶

Back

Close

Full Screen / Esc

Printer-friendly Version

Interactive Discussion



**SCIAMACHY
WFM-DOAS XCO₂:
comparison with
CarbonTracker**

J. Heymann et al.

Title Page

Abstract

Introduction

Conclusions

References

Tables

Figures

◀

▶

◀

▶

Back

Close

Full Screen / Esc

Printer-friendly Version

Interactive Discussion



Barkley, M. P., Monks, P. S., Hewitt, A. J., Machida, T., Desai, A., Vinnichenko, N., Nakazawa, T., Yu Arshinov, M., Fedoseev, N., and Watai, T.: Assessing the near surface sensitivity of SCIAMACHY atmospheric CO₂ retrieved using (FSI) WFM-DOAS, *Atmos. Chem. Phys.*, 7, 3597–3619, doi:10.5194/acp-7-3597-2007, 2007. 2890

5 Barnes, W., Pagano, T., and Salomonson, V.: Prelaunch characteristics of the Moderate Resolution Imaging Spectroradiometer (MODIS) on EOS-AM1, *IEEE T. Geosci. Remote.*, 36, 1088–1100, doi:10.1109/36.700993, 1998. 2898

Benedetti, A., Morcrette, J.-J., Boucher, O., Dethof, A., Engelen, R.-J., Fisher, M., Flentje, H., Huneus, N., Jones, L., Kaiser, J. W., Kinne, S., Mangold, A., Razinger, M., Simmons, A. J.,
10 and Suttie, M.: Aerosol analysis and forecast in the European Centre for Medium-Range Weather Forecasts Integrated Forecast System: 2. Data assimilation, *J. Geophys. Res.*, 114, D13205, doi:10.1029/2008JD011115, 2009. 2898

Bösch, H., Toon, G. C., Sen, B., Washenfelder, R. A., Wennberg, P. O., Buchwitz, M., de Beek, R., Burrows, J. P., Crisp, D., Christi, M., Connor, B. J., Natraj, V., and Yung, Y. L.: Space-based near-infrared CO₂ measurements: Testing the Orbiting Carbon Observatory retrieval algorithm and validation concept using SCIAMACHY observations over Park Falls, Wisconsin, *J. Geophys. Res.*, 111, D23302, doi:10.1029/2006JD007080, 2006. 2890

Bösch, H., Baker, D., Connor, B., Crisp, D., and Miller, C.: Global Characterization of CO₂ Column Retrievals from Shortwave-Infrared Satellite Observations of the Orbiting Carbon Observatory-2 Mission, *Remote Sens. Environ.*, 3, 270–304, doi:10.3390/rs3020270, 2011. 2890

Bovensmann, H., Burrows, J. P., Buchwitz, M., Frerick, J., Noël, S., Rozanov, V. V., Chance, K. V., and Goede, A.: SCIAMACHY – Mission Objectives and Measurement Modes, *J. Atmos. Sci.*, 56, 127–150, 1999. 2889, 2894

25 Bovensmann, H., Buchwitz, M., Burrows, J. P., Reuter, M., Krings, T., Gerilowski, K., Schneising, O., Heymann, J., Tretner, A., and Erzinger, J.: A remote sensing technique for global monitoring of power plant CO₂ emissions from space and related applications, *Atmos. Meas. Tech.*, 3, 781–811, doi:10.5194/amt-3-781-2010, 2010. 2890

Bril, A., Oshchepkov, S., Yokota, T., and Inoue, G.: Parameterization of aerosol and cirrus cloud effects on reflected sunlight spectra measured from space: application of the equivalence theorem, *Appl. Optics*, 46, 2460–2470, 2007. 2891

30 Buchwitz, M. and Burrows, J. P.: Retrieval of CH₄, CO, and CO₂ total column amounts from SCIAMACHY near-infrared nadir spectra: Retrieval algorithm and first results, in: *Remote*

SCIAMACHY WFM-DOAS XCO₂: comparison with CarbonTracker

J. Heymann et al.

[Title Page](#)
[Abstract](#)
[Introduction](#)
[Conclusions](#)
[References](#)
[Tables](#)
[Figures](#)
[Back](#)
[Close](#)
[Full Screen / Esc](#)
[Printer-friendly Version](#)
[Interactive Discussion](#)


Sensing of Clouds and the Atmosphere VIII, edited by: Schäfer, K. P., Comèron, A., Carleer, M. R., and Picard, R. H., Proc. SPIE, 5235, 375–388, 2004. 2890, 2891, 2892, 2899

Buchwitz, M., Rozanov, V. V., and Burrows, J. P.: A near-infrared optimized DOAS method for the fast global retrieval of atmospheric CH₄, CO, CO₂, H₂O, and N₂O total column amounts from SCIAMACHY Envisat-1 nadir radiances, J. Geophys. Res., 105, 15 231–15 245, 2000. 2890, 2892

Buchwitz, M., de Beek, R., Burrows, J. P., Bovensmann, H., Warneke, T., Notholt, J., Meirink, J. F., Goede, A. P. H., Bergamaschi, P., Körner, S., Heimann, M., and Schulz, A.: Atmospheric methane and carbon dioxide from SCIAMACHY satellite data: initial comparison with chemistry and transport models, Atmos. Chem. Phys., 5, 941–962, doi:10.5194/acp-5-941-2005, 2005. a. 2890, 2891, 2892, 2894, 2895, 2897

Buchwitz, M., de Beek, R., Noël, S., Burrows, J. P., Bovensmann, H., Bremer, H., Bergamaschi, P., Körner, S., and Heimann, M.: Carbon monoxide, methane and carbon dioxide columns retrieved from SCIAMACHY by WFM-DOAS: year 2003 initial data set, Atmos. Chem. Phys., 5, 3313–3329, doi:10.5194/acp-5-3313-2005, 2005b. 2890, 2892

Buchwitz, M., de Beek, R., Noël, S., Burrows, J. P., Bovensmann, H., Schneising, O., Khlystova, I., Bruns, M., Bremer, H., Bergamaschi, P., Körner, S., and Heimann, M.: Atmospheric carbon gases retrieved from SCIAMACHY by WFM-DOAS: version 0.5 CO and CH₄ and impact of calibration improvements on CO₂ retrieval, Atmos. Chem. Phys., 6, 2727–2751, doi:10.5194/acp-6-2727-2006, 2006. 2890

Buchwitz, M., Schneising, O., Burrows, J. P., Bovensmann, H., Reuter, M., and Notholt, J.: First direct observation of the atmospheric CO₂ year-to-year increase from space, Atmos. Chem. Phys., 7, 4249–4256, doi:10.5194/acp-7-4249-2007, 2007. 2890

Burrows, J. P., Hölzle, E., Goede, A. P. H., Visser, H., and Fricke, W.: SCIAMACHY – Scanning Imaging Absorption Spectrometer for Atmospheric Chartography, Acta Astronaut., 35, 445–451, 1995. 2889

Butz, A., Hasekamp, O. P., Frankenberg, C., and Aben, I.: Retrievals of atmospheric CO₂ from simulated space-borne measurements of backscattered near-infrared sunlight: accounting for aerosol effects, Appl. Optics, 48, 3322–3336, 2009. 2890, 2891

Butz, A., Guerlet, S., Hasekamp, O., Schepers, D., Galli, A., Aben, I., Frankenberg, C., Hartmann, J.-M., Tran, H., Kuze, A., Keppel-Aleks, G., Toon, G., Wunch, D., Wennberg, P., Deutscher, N., Griffith, D., Macatangay, R., Messerschmidt, J., Notholt, J., and Warneke, T.:

**SCIAMACHY
WFM-DOAS XCO₂:
comparison with
CarbonTracker**

J. Heymann et al.

[Title Page](#)
[Abstract](#)
[Introduction](#)
[Conclusions](#)
[References](#)
[Tables](#)
[Figures](#)
[⏪](#)
[⏩](#)
[◀](#)
[▶](#)
[Back](#)
[Close](#)
[Full Screen / Esc](#)
[Printer-friendly Version](#)
[Interactive Discussion](#)

Toward accurate CO₂ and CH₂ observations from GOSAT, *Geophys. Res. Lett.*, 38, L14812, doi:10.1029/2011GL047888, 2011. 2891

Chevallier, F., Bréon, F.-M., and Rayner, P. J.: Contribution of the Orbiting Carbon Observatory to the estimation of CO₂ sources and sinks: Theoretical study in a variational data assimilation framework, *J. Geophys. Res.*, 112, D09307, doi:10.1029/2006JD007375, 2007. 2889

Christi, M. J. and Stephens, G. L.: Retrieving profiles of atmospheric CO₂ in clear sky and in the presence of thin cloud using spectroscopy from the near and thermal infrared: a preliminary case study, *J. Geophys. Res.*, 109, D04316, doi:10.1029/2003JD004058, 2004. 2891

Crisp, D., Atlas, R. M., Bréon, F.-M., Brown, L. R., Burrows, J. P., Ciais, P., Connor, B. J., Doney, S. C., Fung, I. Y., Jacob, D. J., Miller, C. E., O'Brien, D., Pawson, S., Randerson, J. T., Rayner, P., Salawitch, R. S., Sander, S. P., Sen, B., Stephens, G. L., Tans, P. P., Toon, G. C., Wennberg, P. O., Wofsy, S. C., Yung, Y. L., Kuang, Z., Chudasama, B., Sprague, G., Weiss, P., Pollock, R., Kenyon, D., and Schroll, S.: The Orbiting Carbon Observatory (OCO) mission, *Adv. Space Res.*, 34, 700–709, 2004. 2890

Dufour, E. and Bréon, F.-M.: Spaceborn estimate of atmospheric CO₂ column by use of the differential absorption method: error analysis, *Appl. Optics*, 42, 3595–3609, 2003. 2891

Heymann, J., Schneising, O., Reuter, M., Buchwitz, M., Bovensmann, H., and Burrows, J. P.: SCIAMACHY WFM-DOAS XCO₂: Reduction of scattering related errors, in preparation, 2012. 2907

Houweling, S., Breon, F.-M., Aben, I., Rödenbeck, C., Gloor, M., Heimann, M., and Ciais, P.: Inverse modeling of CO₂ sources and sinks using satellite data: a synthetic inter-comparison of measurement techniques and their performance as a function of space and time, *Atmos. Chem. Phys.*, 4, 523–538, doi:10.5194/acp-4-523-2004, 2004. 2889

Houweling, S., Hartmann, W., Aben, I., Schrijver, H., Skidmore, J., Roelofs, G.-J., and Breon, F.-M.: Evidence of systematic errors in SCIAMACHY-observed CO₂ due to aerosols, *Atmos. Chem. Phys.*, 5, 3003–3013, doi:10.5194/acp-5-3003-2005, 2005. 2890, 2891

Keppel-Aleks, G., Wennberg, P. O., Washenfelder, R. A., Wunch, D., Schneider, T., Toon, G. C., Andres, R. J., Blavier, J.-F., Connor, B., Davis, K. J., Desai, A. R., Messerschmidt, J., Notholt, J., Roehl, C. M., Sherlock, V., Stephens, B. B., Vay, S. A., and Wofsy, S. C.: The imprint of surface fluxes and transport on variations in total column carbon dioxide, *Biogeosciences*, 9, 875–891, doi:10.5194/bg-9-875-2012, 2012. 2904

**SCIAMACHY
WFM-DOAS XCO₂:
comparison with
CarbonTracker**

J. Heymann et al.

Title Page

Abstract

Introduction

Conclusions

References

Tables

Figures

◀

▶

◀

▶

Back

Close

Full Screen / Esc

Printer-friendly Version

Interactive Discussion



Kuang, Z., Margolis, J., Toon, G., Crisp, D., and Yung, Y.: Spaceborne measurements of atmospheric CO₂ by high-resolution NIR spectrometry of reflected sunlight: an introductory study, *Geophys. Res. Lett.*, 29, 1716, doi:10.1029/2001GL014298, 2002. 2890

Kuze, A., Suto, H., Nakajima, M., and Hamazaki, T.: Thermal and near infrared sensor for carbon observation Fourier-transform spectrometer on the Greenhouse Gases Observing Satellite for greenhouse gases monitoring, *Appl. Optics*, 48, 6716–6733, 2009. 2890

Mao, J. and Kawa, S. R.: Sensitivity studies for space-based measurement of atmospheric total column carbon dioxide by reflected sunlight, *Appl. Optics*, 43, 914–927, 2004. 2891

Miller, C. E., Crisp, D., DeCola, P. L., Olsen, S. C., Randerson, J. T., Michalak, A. M., Alkhaled, A., Rayner, P., Jacob, D. J., Suntharalingam, P., Jones, D. B. A., Denning, A. S., Nicholls, M. E., Doney, S. C., Pawson, S., Boesch, H., Connor, B. J., Fung, I. Y., O'Brien, D., Salawitch, R. J., Sander, S. P., Sen, B., Tans, P., Toon, G. C., Wennberg, P. O., Wofsy, S. C., Yung, Y. L., and Law, R. M.: Precision requirements for space-based X_{CO₂} data, *J. Geophys. Res.*, 112, D10314, doi:10.1029/2006JD007659, 2007. 2889

Morcrette, J.-J., Boucher, O., Jones, L., Salmond, D., Bechtold, P., Beljaars, A., Benedetti, A., Bonet, A., Kaiser, W., Razinger, M., Schulz, M., Serrar, S., Simmons, A. J., Sofiev, M., Suttie, M., Tompkins, A., and Untch, A.: Aerosol analysis and forecast in the European Centre for Medium-Range Weather Forecasts Integrated Forecast System: Forward modeling, *J. Geophys. Res.*, 114, D06206, doi:10.1029/2008JD011235, 2009. 2898

Morino, I., Uchino, O., Inoue, M., Yoshida, Y., Yokota, T., Wennberg, P. O., Toon, G. C., Wunch, D., Roehl, C. M., Notholt, J., Warneke, T., Messerschmidt, J., Griffith, D. W. T., Deutscher, N. M., Sherlock, V., Connor, B., Robinson, J., Sussmann, R., and Rettinger, M.: Preliminary validation of column-averaged volume mixing ratios of carbon dioxide and methane retrieved from GOSAT short-wavelength infrared spectra, *Atmos. Meas. Tech.*, 4, 1061–1076, doi:10.5194/amt-4-1061-2011, 2011. 2890

O'Brien, D. M. and Rayner, P. J.: Global observations of the carbon budget 2. CO₂ column from differential absorption of reflected sunlight in the 1.61 μm band of CO₂, *J. Geophys. Res.*, 107, 4354, doi:10.1029/2001JD000617, 2002. 2890

Oshchepkov, S., Bril, A., and Yokota, T.: PPDF-based method to account for atmospheric light scattering in observations of carbon dioxide from space, *J. Geophys. Res.-Atmos.*, 113, D23210, doi:10.1029/2008JD010061, 2008. 2890

Peters, W., Jacobson, A. R., Sweeney, C., Andrews, A. E., Conway, T. J., Masarie, K., Miller, J. B., Bruhwiler, L. M. P., Petron, G., Hirsch, A. I., Worthy, D. E. J., van der Werf, G. R.,

**SCIAMACHY
WFM-DOAS XCO₂:
comparison with
CarbonTracker**

J. Heymann et al.

Title Page

Abstract

Introduction

Conclusions

References

Tables

Figures

⏪

⏩

◀

▶

Back

Close

Full Screen / Esc

Printer-friendly Version

Interactive Discussion



Randerson, J. T., Wennberg, P. O., Krol, M. C., and Tans, P. P.: An atmospheric perspective on North American carbon dioxide exchange: CarbonTracker, *P. Natl. Acad. Sci.*, 104, 18925–18930, doi:10.1073/pnas.0708986104, 2007. 2897

Rayner, P. J. and O'Brien, D. M.: The utility of remotely sensed CO₂ concentration data in surface inversions, *Geophys. Res. Lett.*, 28, 175–178, 2001. 2889

Reuter, M., Buchwitz, M., Schneising, O., Heymann, J., Bovensmann, H., and Burrows, J. P.: A method for improved SCIAMACHY CO₂ retrieval in the presence of optically thin clouds, *Atmos. Meas. Tech.*, 3, 209–232, doi:10.5194/amt-3-209-2010, 2010. 2890, 2891

Reuter, M., Bovensmann, H., Buchwitz, M., Burrows, J. P., Connor, B. J., Deutscher, N. M., Griffith, D. W. T., Heymann, J., Keppel-Aleks, G., Messerschmidt, J., Notholt, J., Petri, C., Robinson, J., Schneising, O., Sherlock, V., Velazco, V., Warneke, T., Wennberg, P. O., and Wunch, D.: Retrieval of atmospheric CO₂ with enhanced accuracy and precision from SCIAMACHY: Validation with FTS measurements and comparison with model results, *J. Geophys. Res.*, 116, D04301, doi:10.1029/2010JD015047, 2011. 2891

Rozanov, A., Rozanov, V., Buchwitz, M., Kokhanovsky, A., and Burrows, J.: SCIAMACHY 2.0 – A new radiative transfer model for geophysical applications in the 175–2400 nm spectral region, in: *Atmospheric remote sensing: Earth's surface, troposphere, stratosphere and mesosphere – I*, edited by: Burrows, J. and Eichmann, K., vol. 36 of *Adv. Space Res.*, doi:10.1016/j.asr.2005.03.012, 35th COSPAR Scientific Assembly, 18–25 July 2004, Paris, France, 1015–1019, 2005. 2895

Rozanov, V. V. and Rozanov, A. V.: Differential optical absorption spectroscopy (DOAS) and air mass factor concept for a multiply scattering vertically inhomogeneous medium: theoretical consideration, *Atmos. Meas. Tech.*, 3, 751–780, doi:10.5194/amt-3-751-2010, 2010. 2892

Saito, N., Imasu, R., Ota, Y., and Niwa, Y.: CO₂ retrieval algorithm for the thermal infrared spectra of the Greenhouse Gases Observing Satellite: Potential of retrieving CO₂ vertical profile from high-resolution FTS sensor, *J. Geophys. Res.*, 114, D17305, doi:10.1029/2008JD011500, 2009. 2890

Schneising, O., Buchwitz, M., Burrows, J. P., Bovensmann, H., Reuter, M., Notholt, J., Macatangay, R., and Warneke, T.: Three years of greenhouse gas column-averaged dry air mole fractions retrieved from satellite – Part 1: Carbon dioxide, *Atmos. Chem. Phys.*, 8, 3827–3853, doi:10.5194/acp-8-3827-2008, 2008. 2890, 2891, 2892, 2893, 2894, 2896, 2905

SCIAMACHY WFM-DOAS XCO₂: comparison with CarbonTracker

J. Heymann et al.

[Title Page](#)
[Abstract](#)
[Introduction](#)
[Conclusions](#)
[References](#)
[Tables](#)
[Figures](#)
[⏪](#)
[⏩](#)
[◀](#)
[▶](#)
[Back](#)
[Close](#)
[Full Screen / Esc](#)
[Printer-friendly Version](#)
[Interactive Discussion](#)


- Schneising, O., Buchwitz, M., Burrows, J. P., Bovensmann, H., Bergamaschi, P., and Peters, W.: Three years of greenhouse gas column-averaged dry air mole fractions retrieved from satellite - Part 2: Methane, *Atmos. Chem. Phys.*, 9, 443–465, 2009. 2892, 2896
- Schneising, O., Buchwitz, M., Reuter, M., Heymann, J., Bovensmann, H., and Burrows, J. P.: Long-term analysis of carbon dioxide and methane column-averaged mole fractions retrieved from SCIAMACHY, *Atmos. Chem. Phys.*, 11, 2863–2880, doi:10.5194/acp-11-2863-2011, 2011. 2890, 2891, 2892, 2893, 2904, 2905, 2906
- Schneising, O., Bergamaschi, P., Bovensmann, H., Buchwitz, M., Burrows, J. P., Deutscher, N. M., Griffith, D. W. T., Heymann, J., Macatangay, R., Messerschmidt, J., Notholt, J., Rettinger, M., Reuter, M., Sussmann, R., Velazco, V. A., Warneke, T., Wennberg, P. O., and Wunch, D.: Atmospheric greenhouse gases retrieved from SCIAMACHY: comparison to ground-based FTS measurements and model results, *Atmos. Chem. Phys.*, 12, 1527–1540, doi:10.5194/acp-12-1527-2012, 2012. 2890, 2891, 2903
- Solomon, S., Qin, D., Manning, M., Chen, Z., Marquis, M., Averyt, K. B., Tignor, M., and Miller, H. L. (Eds.): *Climate change 2007: The physical science basis, Contribution of working group I to the Fourth Assessment Report of the Intergovernmental Panel on Climate Change – IPCC*, Cambridge University Press, 2007. 2889
- Stephens, B. B., Gurney, K. R., Tans, P. P., Sweeney, C., Peters, W., Bruhwiler, L., Ciais, P., Ramonet, M., Bousquet, P., Nakazawa, T., Aoki, S., Machida, T., Inoue, G., Vinnichenko, N., Lloyd, J., Jordan, A., Heimann, M., Shibistova, O., Langenfelds, R. L., Steele, L. P., Francey, R. J., and Denning, A. S.: Weak northern and strong tropical land carbon uptake from vertical profiles of atmospheric CO₂, *Science*, 316, 1732–1735, doi:10.1126/science.1137004, 2007. 2889
- Tilstra, L. G., de Graaf, M., Aben, I., and Stammes, P.: Analysis of 5 years of SCIAMACHY absorbing aerosol index data, *Proceedings ENVISAT Symposium, Montreux, Switzerland, ESA Special Publication SP-636*, 2007. 2893
- Tolton, B. T. and Plouffe, D.: Sensitivity of radiometric measurements of the atmospheric CO₂ column from space, *Appl. Optics*, 40, 1305–1313, 2001. 2890
- van Diedenhoven, B., Hasekamp, O. P., and Aben, I.: Surface pressure retrieval from SCIAMACHY measurements in the O₂ A Band: validation of the measurements and sensitivity on aerosols, *Atmos. Chem. Phys.*, 5, 2109–2120, doi:10.5194/acp-5-2109-2005, 2005. 2891
- Vaughan, M., Young, S., Winker, D., Powell, K., Omar, A., Liu, Z., Yongxiang, H., and Hostetler, C.: Fully automated analysis of space-based lidar data: an overview of the CALIPSO

**SCIAMACHY
WFM-DOAS XCO₂:
comparison with
CarbonTracker**

J. Heymann et al.

Title Page

Abstract

Introduction

Conclusions

References

Tables

Figures

⏪

⏩

◀

▶

Back

Close

Full Screen / Esc

Printer-friendly Version

Interactive Discussion



retrieval algorithms and data products, *Laser Radar Tech. Atmos. Sens.*, 5575, 16–30, doi:10.1117/12.572024, 2004. 2898

Velazco, V. A., Buchwitz, M., Bovensmann, H., Reuter, M., Schneising, O., Heymann, J., Krings, T., Gerilowski, K., and Burrows, J. P.: Towards space based verification of CO₂ emissions from strong localized sources: fossil fuel power plant emissions as seen by a CarbonSat constellation, *Atmos. Meas. Tech.*, 4, 2809–2822, doi:10.5194/amt-4-2809-2011, 2011. 2890

Winker, D., Vaughan, M., Omar, A., Hu, Y., Powell, K. A., Liu, Z., Hunt, W., and Young, S.: Overview of the CALIPSO Mission and CALIOP Data Processing Algorithms, *J. Atmos. Ocean. Tech.*, 26, 2310–2323, 2009. 2898

Winker, D. M., Hunt, W. H., and McGill, M. J.: Initial performance assessment of CALIOP, *Geophys. Res. Lett.*, 34, L19803, doi:doi:10.1029/2007GL030135, 2007. 2898

Yang, Z., Washenfelder, R. A., Keppel-Aleks, G., Krakauer, N. Y., Randerson, J. T., Tans, P. P., Sweeney, C., and Wennberg, P. O.: New constraints on Northern Hemisphere growing season net flux, *Geophys. Res. Lett.*, 34, L12807, doi:10.1029/2007GL029742, 2007. 2904

Yokota, T., Oguma, H., Morino, I., and Inoue, G.: A nadir looking SWIR sensor to monitor CO₂ column density for Japanese GOSAT project, *Proceedings of the twenty-fourth international symposium on space technology and science, Miyazaki: Japan Society for Aeronautical and Space Sciences and ISTS*, 887–889, 2004. 2890

Yoshida, Y., Ota, Y., Eguchi, N., Kikuchi, N., Nobuta, K., Tran, H., Morino, I., and Yokota, T.: Retrieval algorithm for CO₂ and CH₄ column abundances from short-wavelength infrared spectral observations by the Greenhouse gases observing satellite, *Atmos. Meas. Tech.*, 4, 717–734, doi:10.5194/amt-4-717-2011, 2011. 2890

**SCIAMACHY
WFM-DOAS XCO₂:
comparison with
CarbonTracker**

J. Heymann et al.

Table 1. Minimum detectable effective cloud optical depth (eCOD) for the PMD and O₂ based WFM-DOAS cloud detection algorithms for various scenarios as defined by surface albedo and solar zenith angle (SZA). The following settings have been used for all scenarios: aerosols: default scenario (see main text); clouds: cloud geometrical thickness CGT = 0.5 km and cloud fractional coverage CFC = 1.0. “∞” means that even clouds with large eCOD are not detected. “0.00” means that clouds are “detected” even if the scene is cloud free.

Scenario Albedo/SZA	Minimum effective COD			
		CTH [km]		
		4	10	16
0.1/20°	PMD:	1.16	1.20	1.23
	O ₂ :	0.34	0.10	0.07
0.1/40°	PMD:	0.89	0.89	0.89
	O ₂ :	0.23	0.07	0.04
0.1/60°	PMD:	0.42	0.40	0.39
	O ₂ :	0.11	0.03	0.02
Gras/40°	PMD:	1.32	1.32	1.32
	O ₂ :	1.00	0.28	0.18
Sand/40°	PMD:	1.27	1.26	1.26
	O ₂ :	0.08	0.02	0.02
Water/40°	PMD:	1.43	1.42	1.42
	O ₂ :	0.53	0.15	0.10
Snow/40°	PMD:	0.00	0.00	0.00
	O ₂ :	∞	0.69	0.43

Title Page

Abstract

Introduction

Conclusions

References

Tables

Figures

◀

▶

◀

▶

Back

Close

Full Screen / Esc

Printer-friendly Version

Interactive Discussion



**SCIAMACHY
WFM-DOAS XCO₂:
comparison with
CarbonTracker**

J. Heymann et al.

Title Page

Abstract

Introduction

Conclusions

References

Tables

Figures

◀

▶

◀

▶

Back

Close

Full Screen / Esc

Printer-friendly Version

Interactive Discussion

**Table 2.** Latitudes and longitudes of the regions used in this study (see also Fig. 8).

Region	ID	Latitude Range		Longitude Range	
Northern Hemisphere	NH	0°	– 90°	–180°	– 180°
Western USA	WUS	25°	– 50°	–125°	– –100°
Eastern USA	EUS	25°	– 50°	–98°	– –67°
Park Falls	PF	38°	– 50°	–95°	– –85°
Europe	EU	35°	– 70°	–10°	– 30°
Northern Africa	AF	4°	– 30°	–20°	– 0°
Arabia	AR	10°	– 35°	35°	– 60°
Russia	RUS	45°	– 70°	35°	– 130°
India	IN	5°	– 30°	65°	– 90°
China	CN	20°	– 43°	100°	– 123°
Southern Hemisphere	SH	–90°	– 0°	–180°	– 180°
South America	SAM	–30°	– 0°	–81°	– –35°
Southern Africa	SAF	–35°	– 0°	8°	– 51°
Australia	AU	–43°	– –10°	110°	– 156°
Darwin	DW	–20°	– –12°	127°	– 142°
Global	G	–90°	– 90°	–180°	– 180°

Table 3. Results of the comparison of the scan-angle-bias corrected (S^*) and uncorrected (S) SCIAMACHY WFMDv2.1 XCO_2 with CarbonTracker (C). Listed are correlation coefficients (r , left) and standard deviations (right). *Italic correlation coefficients are non-significant* (see Sect. 6.1). The results shown are based on monthly data.

Region	Correlation of ΔXCO_2^{S-C} with		Standard deviation [ppm]		
	$\Delta XCO_2^{S^*-C}$	$\Delta XCO_2^{S^*-S}$	ΔXCO_2^{S-C}	$\Delta XCO_2^{S^*-C}$	$\Delta XCO_2^{S^*-S}$
NH	0.90	<i>0.04</i>	1.11	1.26	0.56
WUS	0.82	-0.30	1.86	1.85	1.10
EUS	0.84	-0.82	2.77	1.72	1.63
PF	0.68	-0.86	2.51	1.30	1.88
EU	0.84	<i>0.01</i>	1.43	1.72	0.94
AF	0.77	-0.64	1.17	0.90	0.75
AR	0.90	-0.45	1.59	1.42	0.68
RUS	0.80	-0.58	2.00	1.62	1.19
IN	0.99	-0.85	4.86	3.97	1.10
CN	0.93	<i>-0.19</i>	2.11	2.11	0.81
SH	0.90	-0.82	1.62	1.06	0.82
SAM	0.92	-0.67	1.96	1.54	0.80
SAF	0.89	-0.76	1.49	1.05	0.73
AU	0.71	-0.80	1.87	1.14	1.34
DW	0.95	-0.78	4.00	2.99	1.50
G	0.98	-0.23	1.14	1.11	0.22

SCIAMACHY WFM-DOAS XCO_2 : comparison with CarbonTracker

J. Heymann et al.

Title Page

Abstract

Introduction

Conclusions

References

Tables

Figures

⏪

⏩

◀

▶

Back

Close

Full Screen / Esc

Printer-friendly Version

Interactive Discussion

**SCIAMACHY
WFM-DOAS XCO₂:
comparison with
CarbonTracker**

J. Heymann et al.

Table 4. Monthly regional-scale scatter (in ppm and %) of the scan-angle-bias corrected (S*) and uncorrected (S) WFMDv2.1 XCO₂ data obtained from analysing all individual XCO₂ retrievals within a radius of 350 km around various locations. The numerical values are the mean standard deviations of all SCIAMACHY retrievals per month (to remove the seasonal cycle).

Monthly regional-scale scatter of the data							
ID	Location	Lat [°]	Lon [°]	XCO ₂ ^S		XCO ₂ ^{S*}	
				[ppm]	[%]	[ppm]	[%]
1	Lamont	36.6	−97.5	9.24	2.43	7.56	1.99
2	Park Falls	46.0	−90.3	9.68	2.54	7.65	2.01
3	Brasilia	−15.8	−47.9	9.75	2.55	8.26	2.16
4	Orleans	48.0	2.1	7.69	2.01	6.28	1.64
5	Garmisch	47.5	11.1	9.53	2.51	8.09	2.14
6	Bialystok	53.2	23.0	7.62	1.99	6.09	1.59
7	Tazirbu	25.7	21.4	5.60	1.47	4.95	1.30
8	Lubumbashi	−11.7	27.5	10.72	2.82	9.09	2.39
9	Khromtau	50.3	58.5	10.77	2.83	9.23	2.43
10	Darwin	−12.4	130.9	9.42	2.47	7.21	1.89
11	Wollongong	−34.4	150.9	9.38	2.47	7.17	1.89
Mean				9.04 ± 1.51	2.37 ± 0.40	7.42 ± 1.29	1.95 ± 0.34

[Title Page](#)
[Abstract](#)
[Introduction](#)
[Conclusions](#)
[References](#)
[Tables](#)
[Figures](#)
[⏪](#)
[⏩](#)
[◀](#)
[▶](#)
[Back](#)
[Close](#)
[Full Screen / Esc](#)
[Printer-friendly Version](#)
[Interactive Discussion](#)

Table 5. Results of the spatial and temporal correlation analysis of $\Delta\text{XCO}_2^{\text{S}^+-\text{C}}$ related to aerosols (AOD) and clouds (eCOD). Italic coefficients are statistically non-significant. The coefficients, which indicate that aerosols or clouds can explain more than 25 % of the variability of $\Delta\text{XCO}_2^{\text{S}^+-\text{C}}$, are shown in bold. The results shown are based on monthly data.

Region	Correlation coefficients r^2 [%]					
	Correlation of $\Delta\text{XCO}_2^{\text{S}^+-\text{C}}$ with	Temporal	Spatial			
			DJF	MAM	JJA	SON
NH	AOD:	<i>1.7</i>	<i>4.9</i>	<i>8.1</i>	<i>19.8</i>	<i>6.5</i>
	eCOD:	<i>0.0</i>	<i>3.9</i>	<i>11.1</i>	<i>4.3</i>	<i>0.1</i>
WUS	AOD:	9.0	1.7	8.4	25.0	5.3
	eCOD:	3.2	4.4	30.3	2.0	6.2
EUS	AOD:	7.5	7.8	1.1	0.8	4.3
	eCOD:	1.7	5.5	0.2	0.8	0.8
PF	AOD:	6.9	1.2	1.1	14.1	9.0
	eCOD:	2.3	0.0	29.7	30.2	32.9
EU	AOD:	0.8	0.7	1.5	0.3	0.6
	eCOD:	0.4	22.4	0.1	3.4	0.3
AF	AOD:	15.0	14.7	6.5	26.1	3.7
	eCOD:	0.5	17.3	38.2	2.5	0.4
AR	AOD:	18.3	0.0	0.3	34.5	0.0
	eCOD:	15.8	6.0	0.0	32.9	2.6
RUS	AOD:	20.3	0.8	14.6	0.4	2.4
	eCOD:	17.4	25.0	7.6	0.3	0.2
IN	AOD:	54.0	8.2	1.5	12.8	21.9
	eCOD:	67.9	2.0	2.5	4.9	6.9
CN	AOD:	0.1	3.1	0.6	14.4	4.2
	eCOD:	9.2	5.6	0.2	4.0	33.2
SH	AOD:	5.0	8.5	12.7	3.4	9.7
	eCOD:	24.1	23.9	16.1	2.2	13.2
SAM	AOD:	19.2	2.5	3.4	9.8	9.5
	eCOD:	42.9	19.5	15.5	1.8	14.8
SAF	AOD:	0.0	20.0	33.6	4.4	18.3
	eCOD:	31.3	40.0	43.5	11.7	38.1
AU	AOD:	0.3	1.4	17.3	36.2	19.0
	eCOD:	28.4	48.4	2.2	0.8	10.2
DW	AOD:	16.7	12.4	3.5	10.3	34.9
	eCOD:	53.7	29.5	30.6	3.4	45.7
G	AOD:	27.5	3.0	8.4	17.1	7.3
	eCOD:	1.9	12.4	11.7	4.4	1.7

**SCIAMACHY
WFM-DOAS XCO₂:
comparison with
CarbonTracker**

J. Heymann et al.

Title Page

Abstract

Introduction

Conclusions

References

Tables

Figures

⏪

⏩

◀

▶

Back

Close

Full Screen / Esc

Printer-friendly Version

Interactive Discussion



**SCIAMACHY
WFM-DOAS XCO₂:
comparison with
CarbonTracker**

J. Heymann et al.

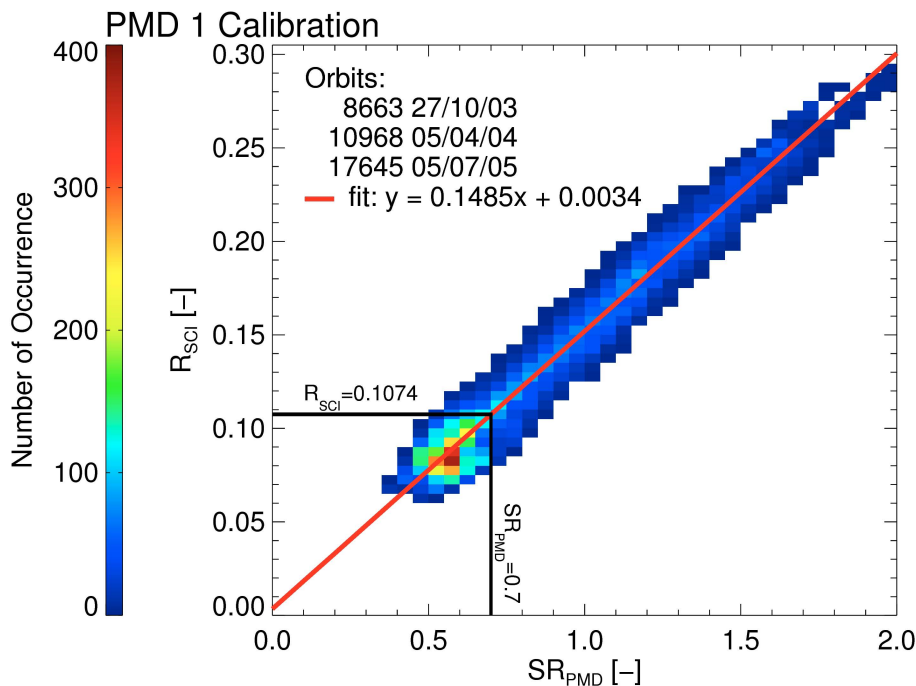


Fig. 1. Calibration of the SCIAMACHY Polarisation Measurement Device number 1 (PMD 1) signal, covering the spectral region 310–365 nm based on three orbits (see annotation). SR_{PMD} is the uncalibrated normalised PMD 1 signal divided by the cosine of the solar zenith angle (SZA). R_{SCI} is the mean reflectivity (sun-normalised radiance divided by the cosine of the SZA) as measured by SCIAMACHY in a spectral region which corresponds to the spectral region covered by PMD 1. The linear fit shows that the PMD 1 based cloud detection criterion $SR_{PMD} = 0.7$ corresponds to $R_{SCI} = 0.1074$.

Title Page

Abstract

Introduction

Conclusions

References

Tables

Figures

◀

▶

◀

▶

Back

Close

Full Screen / Esc

Printer-friendly Version

Interactive Discussion

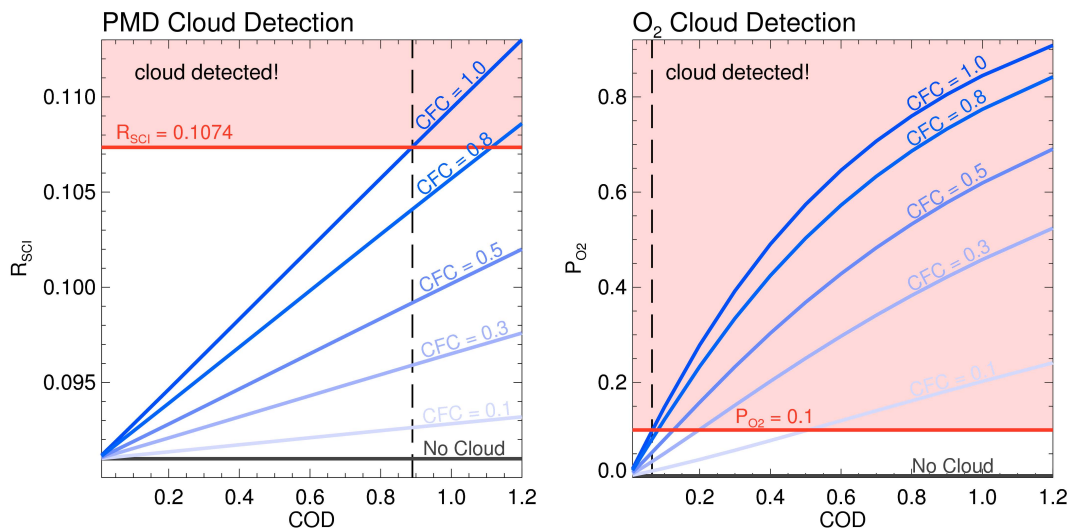


Fig. 2. PMD (given as reflectivity, left panel) and O₂ (right panel) cloud detection thresholds (red lines) compared to results obtained from radiative transfer simulations and simulated retrievals for various cloud scenarios. The left panel shows simulated reflectivity R_{SCI} for the spectral region covered by PMD 1, as a function of cloud optical depth (COD) for different cloud fractional coverages (CFC). The results are valid for a surface albedo of 0.1, the default aerosol scenario, a cloud top height (CTH) of 10 km and a cloud geometrical thickness (CGT) of 0.5 km. The red line shows the PMD cloud detection criterion of $R_{\text{SCI}} = 0.1074$ and the black dashed line shows the minimum detectable COD for CFC = 1.0. The panel on the right shows the simulated deviation of the retrieved O₂-column to the a-priori O₂-column, i.e. P_{O_2} , for the same parameters as used for the left hand side. The red line shows the O₂ cloud detection threshold $P_{\text{O}_2} = 0.1$ and the black dashed line shows the minimum detectable COD for CFC = 1.0.

[Title Page](#)
[Abstract](#)
[Introduction](#)
[Conclusions](#)
[References](#)
[Tables](#)
[Figures](#)
[◀](#)
[▶](#)
[◀](#)
[▶](#)
[Back](#)
[Close](#)
[Full Screen / Esc](#)
[Printer-friendly Version](#)
[Interactive Discussion](#)

CarbonTracker XCO₂

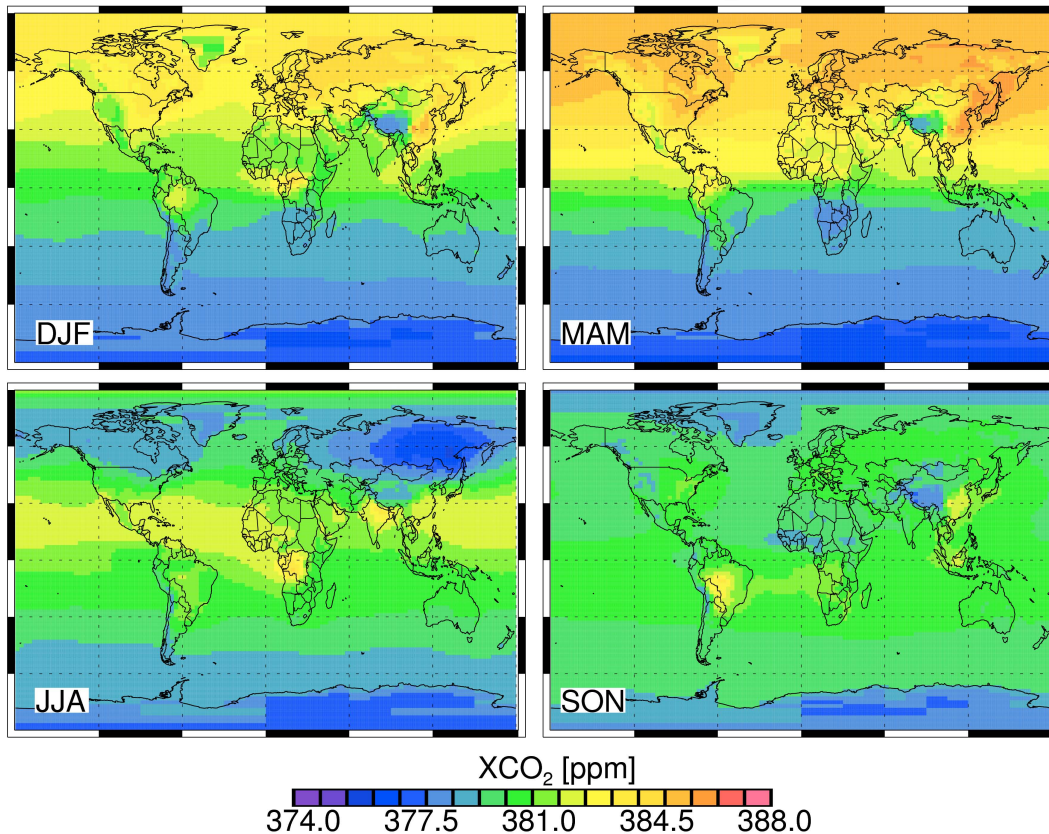


Fig. 3. Seasonal averages of NOAA's CarbonTracker XCO₂ for 2004–2008, modified to take SCIAMACHY's CO₂ column averaging kernels into account.

GEMS – AOD at 760nm

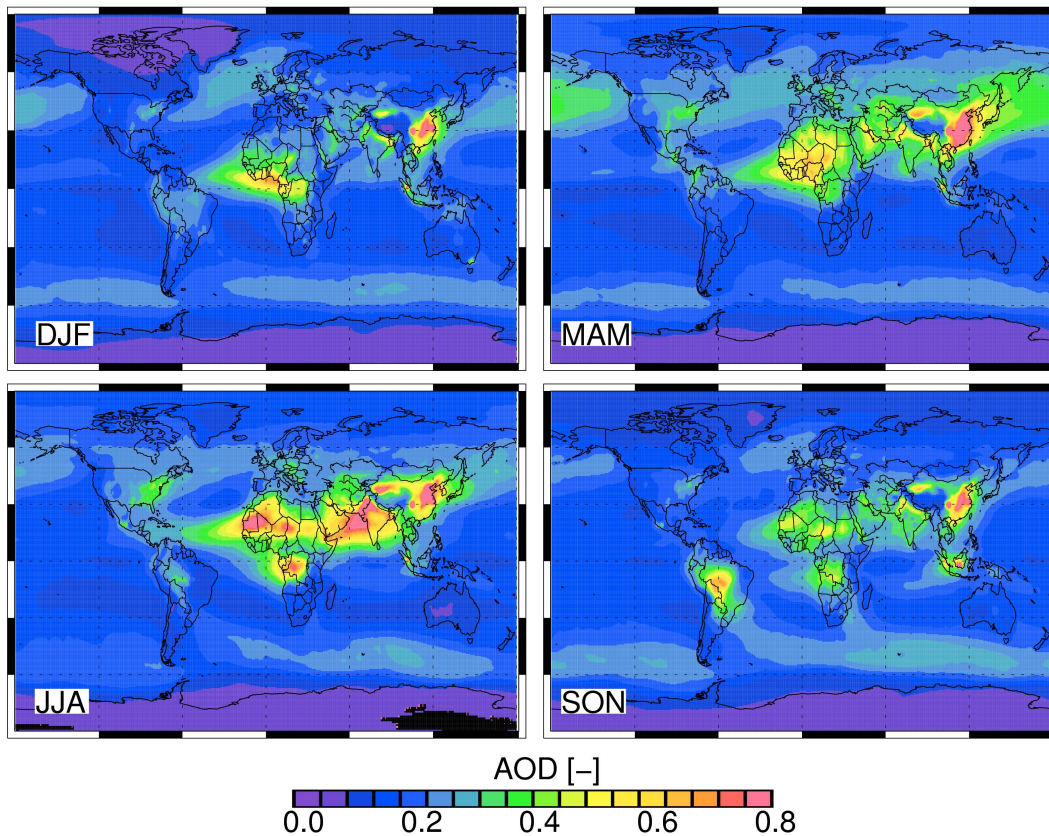


Fig. 4. Seasonal averages of aerosol optical depth (AOD) at 760nm based on the GEMS aerosol data product of the years 2004–2008.

CALIPSO – eCOD

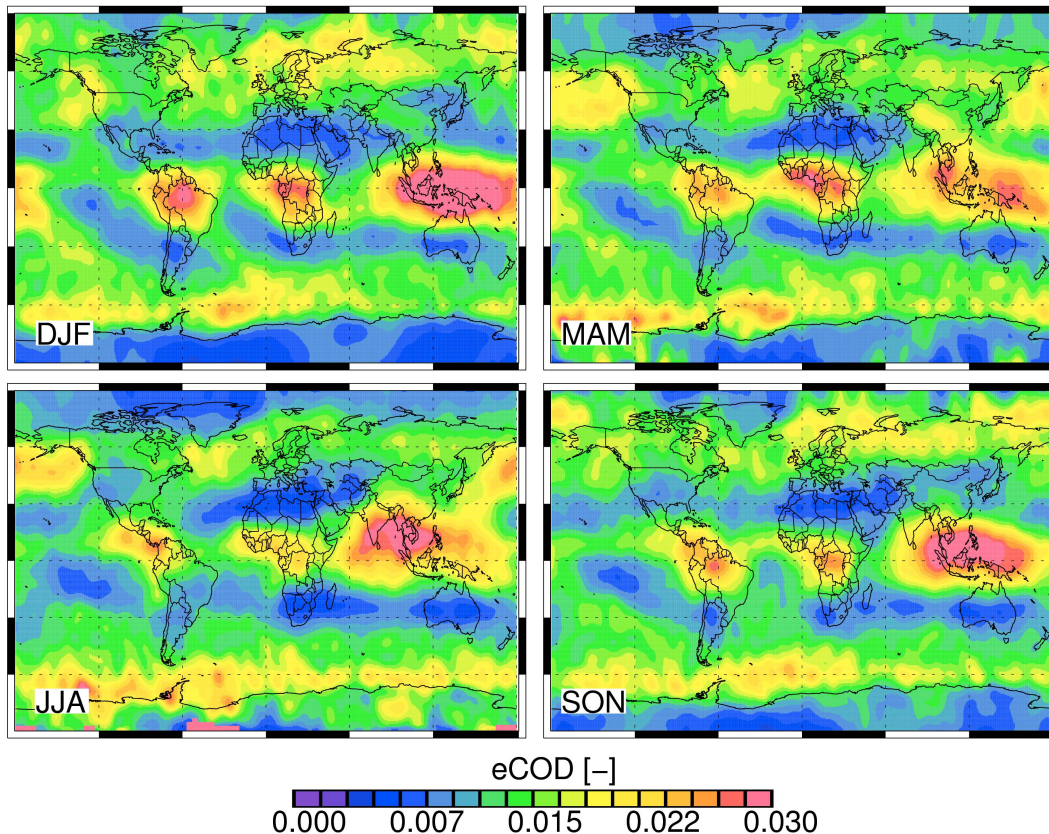


Fig. 5. Seasonal averages of effective cloud optical depth (eCOD) obtained from 2007/2008 CALIPSO/CALIOP data for clouds with COD less than 0.1.

**SCIAMACHY
WFM-DOAS XCO₂:
comparison with
CarbonTracker**

J. Heymann et al.

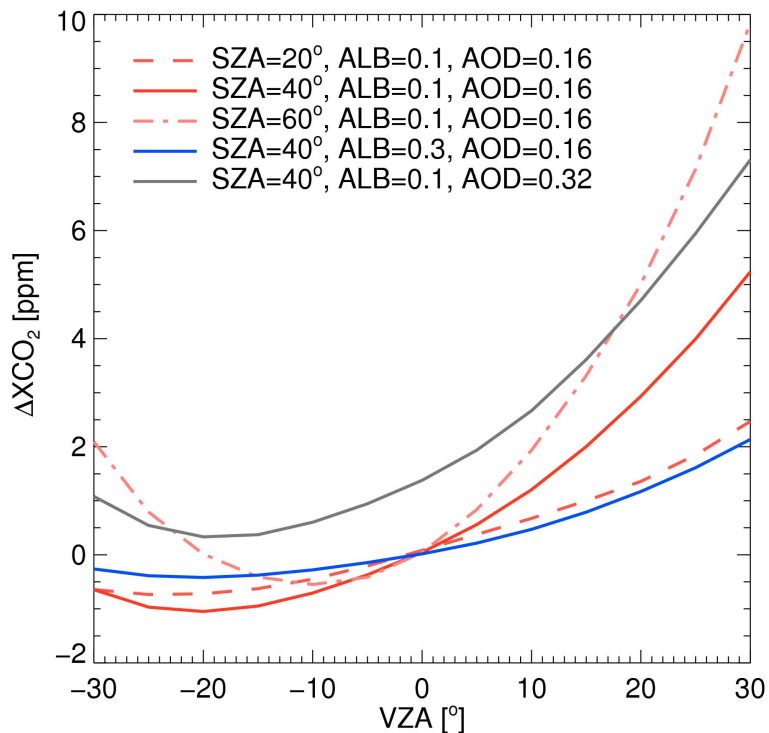


Fig. 6. Simulated systematic WFM-DOAS XCO₂ errors (ΔXCO_2) for different viewing zenith angles (VZA). The simulations are for scenarios with different solar zenith angles (SZA), surface albedos (ALB) and aerosol optical depths (AOD) at 550 nm.

SCIAMACHY WFM-DOAS XCO₂: comparison with CarbonTracker

J. Heymann et al.

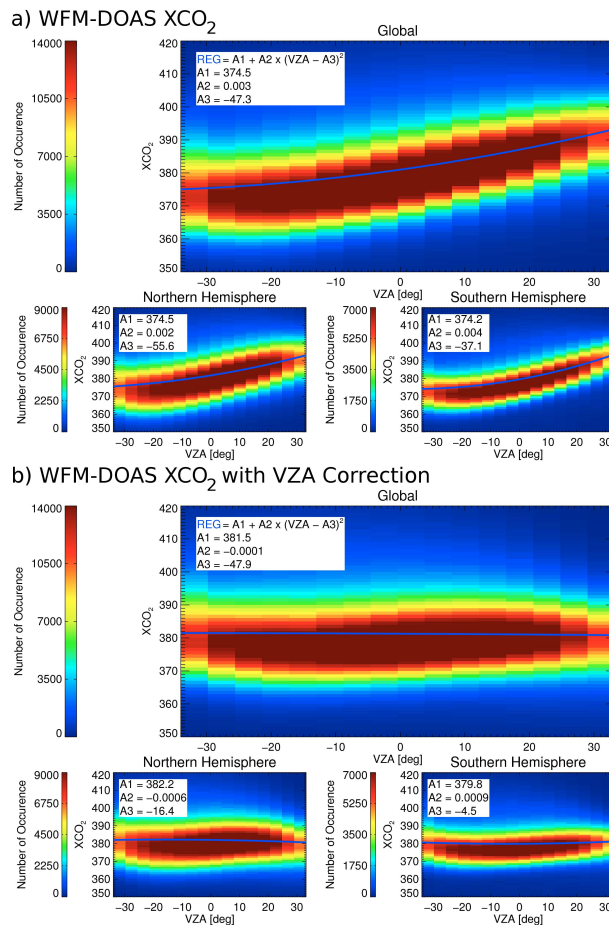


Fig. 7. WFM-DOAS XCO₂ v2.1 VZA dependency before **(a)** and after **(b)** the scan-angle-bias correction. **(a)** 2-D-histogram of WFMDOAS v2.1 XCO₂ versus the VZA using all data between 2003 and 2009. The blue curve is a quadratic fit. **(b)** As **(a)** but after the bias correction.

SCIAMACHY WFM-DOAS XCO₂: comparison with CarbonTracker

J. Heymann et al.

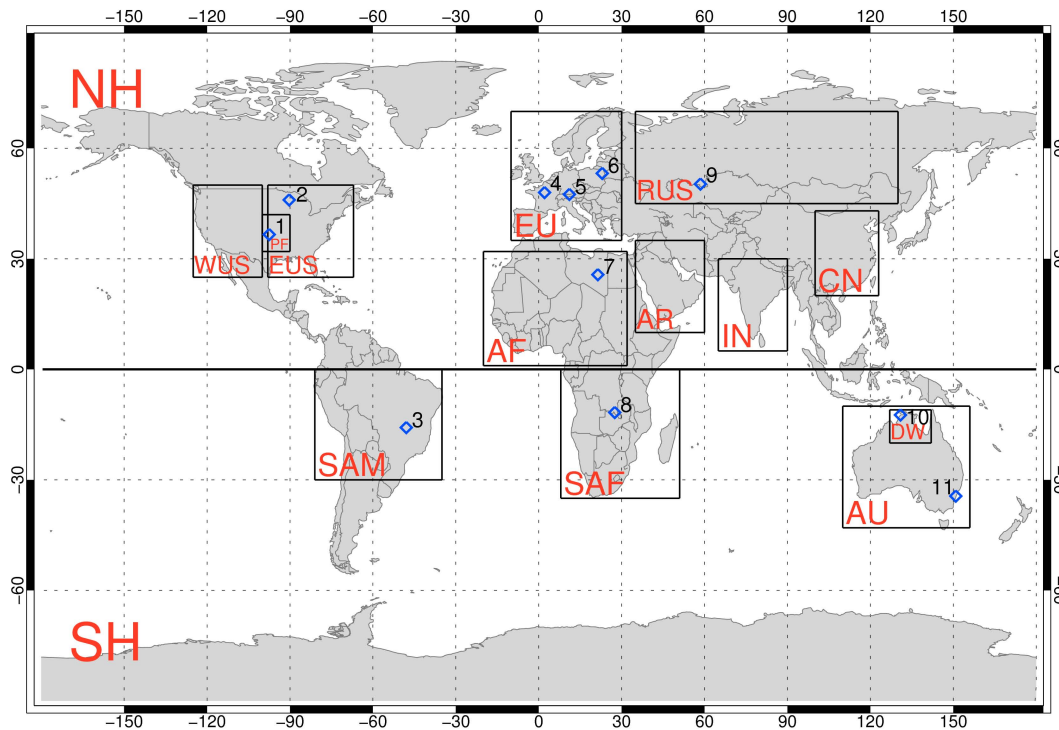


Fig. 8. Regions and locations analysed in this study (see also Tables 2 and 4).

Title Page

Abstract

Introduction

Conclusions

References

Tables

Figures

⏪

⏩

◀

▶

Back

Close

Full Screen / Esc

Printer-friendly Version

Interactive Discussion



Southern Africa

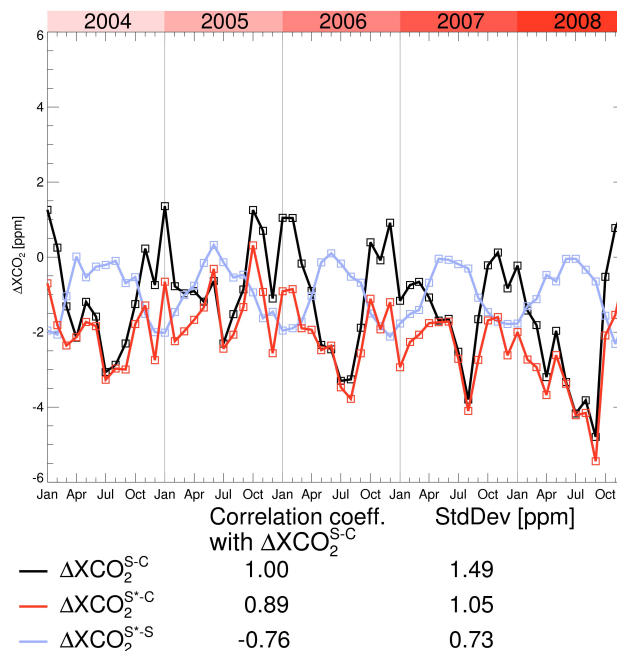


Fig. 9. Results of the comparison between CarbonTracker XCO_2 and WFMDv2.1 XCO_2 with and without scan-angle-bias correction for Southern Africa. Top: The difference between WFMDv2.1 XCO_2 and CarbonTracker XCO_2 (ΔXCO_2^{S-C}) is shown in black and the difference between the scan-angle-bias corrected WFMDv2.1 XCO_2 and CarbonTracker XCO_2 (ΔXCO_2^{S+-C}) is shown in red. The light blue curve represents the difference between scan-angle-bias corrected WFMDv2.1 XCO_2 and uncorrected XCO_2 (ΔXCO_2^{S+-S}). Bottom: correlation coefficients (r) between these differences and ΔXCO_2^{S-C} and corresponding standard deviations.

Title Page

Abstract Introduction

Conclusions References

Tables Figures

◀ ▶

◀ ▶

Back Close

Full Screen / Esc

Printer-friendly Version

Interactive Discussion



China

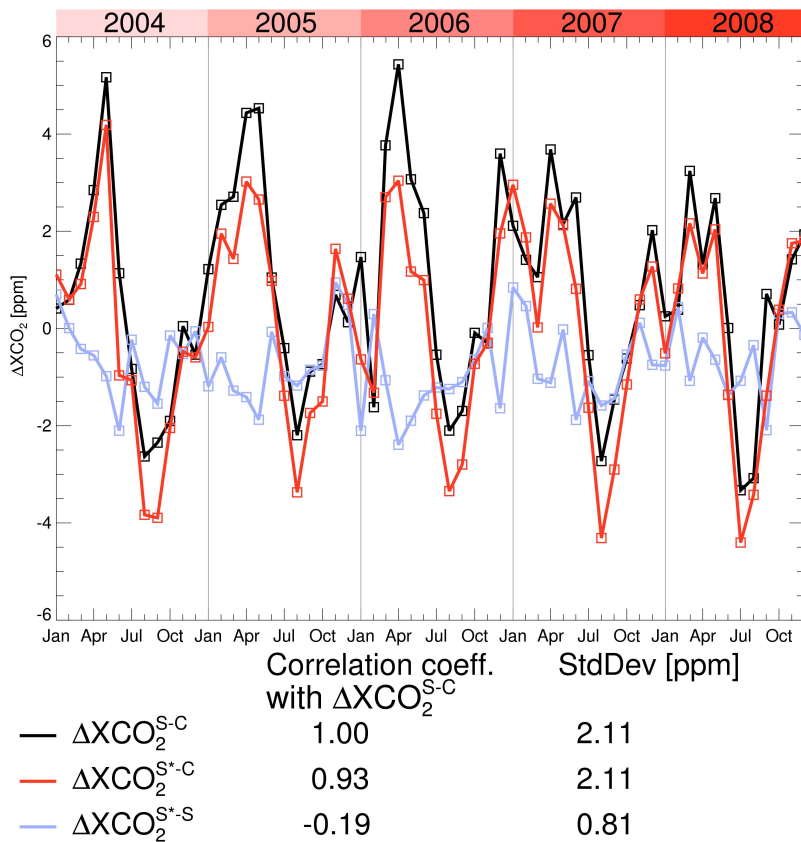


Fig. 10. As Fig. 9 but for China.

[Title Page](#)

[Abstract](#) [Introduction](#)

[Conclusions](#) [References](#)

[Tables](#) [Figures](#)

[⏪](#) [⏩](#)

[◀](#) [▶](#)

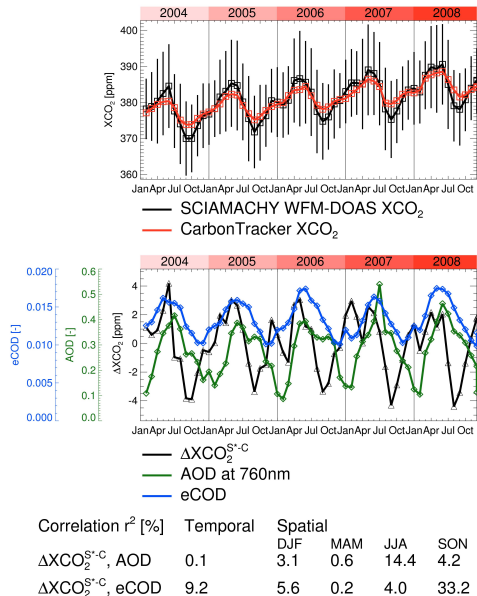
[Back](#) [Close](#)

[Full Screen / Esc](#)

[Printer-friendly Version](#)

[Interactive Discussion](#)

China
a) Temporal



b) Spatial (2004 - 2008)

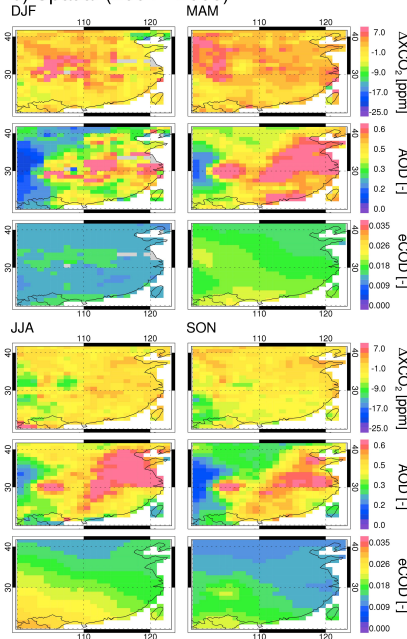
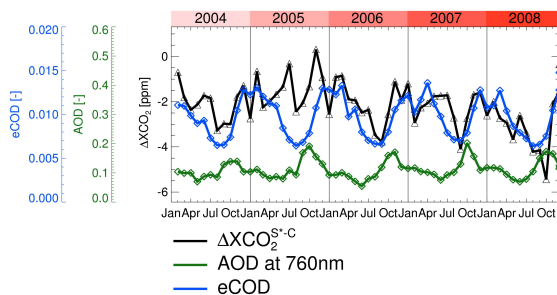
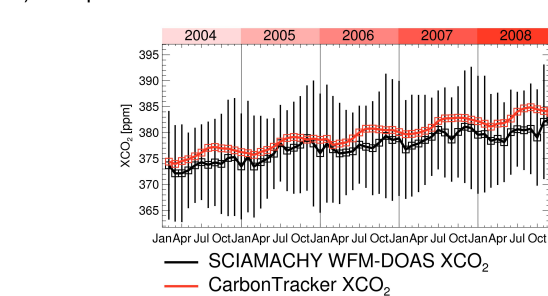


Fig. 11. Results of the temporal and spatial correlation analysis of the difference between scan-angle-corrected SCIAMACHY and CarbonTracker XCO_2 , i.e. ΔXCO_2^{S-C} , and aerosols and thin clouds for China. **(a)** Temporal analysis part: Top: The monthly means and standard deviations of the WFMDOAS XCO_2 are shown in black and CarbonTracker XCO_2 is shown in red. Middle panel: ΔXCO_2^{S-C} (black) compared with GEMS-derived AOD at 760 nm (green) and CALIPSO-derived eCOD (blue). Bottom left panel: The squares of the linear correlation coefficients, r^2 , of the temporal and spatial correlation analysis. **(b)** Spatial analysis part: Three-year seasonal averages of ΔXCO_2^{S-C} , AOD and eCOD.

Southern Africa



Correlation r^2 [%]	Temporal	Spatial			
		DJF	MAM	JJA	SON
ΔXCO_2^{S-C} , AOD	0.0	20.0	33.6	4.4	18.3
ΔXCO_2^{S-C} , eCOD	31.3	40.0	43.5	11.7	38.1

b) Spatial (2004 - 2008)

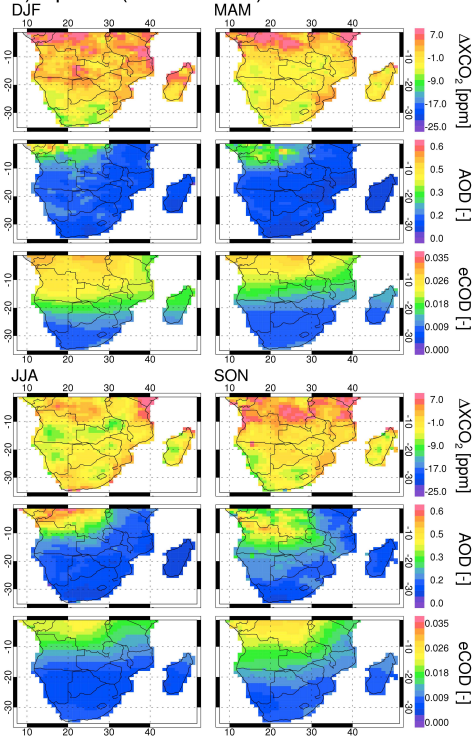


Fig. 12. As Fig. 11 but for Southern Africa.